
Estimating recharge at Yucca Mountain, Nevada, USA: comparison of methods

Alan L. Flint · Lorraine E. Flint
Edward M. Kwicklis · June T. Fabryka-Martin
Gudmundur S. Bodvarsson

Abstract Obtaining values of net infiltration, groundwater travel time, and recharge is necessary at the Yucca Mountain site, Nevada, USA, in order to evaluate the expected performance of a potential repository as a containment system for high-level radioactive waste. However, the geologic complexities of this site, its low precipitation and net infiltration, with numerous mechanisms operating simultaneously to move water through the system, provide many challenges for the estimation of the spatial distribution of recharge. A variety of methods appropriate for arid environments has been applied, including water-balance techniques, calculations using Darcy's law in the unsaturated zone, a soil-physics method applied to neutron-hole water-content data, inverse modeling of thermal profiles in boreholes extending through the thick unsaturated zone, chloride mass balance, atmospheric radionuclides, and empirical approaches. These methods indicate that near-surface infiltration rates at Yucca Mountain are highly variable in time and space, with local (point) values ranging from zero to several hundred millimeters per year. Spatially distributed net-infiltration values average 5 mm/year, with the highest values approaching 20 mm/year near Yucca Crest. Site-scale recharge estimates range from less than 1 to about 12 mm/year. These results have been incorporated into a site-scale model that has been calibrated using these data sets that reflect infiltration processes acting on highly variable temporal and spatial scales. The modeling study predicts highly non-uniform

recharge at the water table, distributed significantly differently from the non-uniform infiltration pattern at the surface.

Résumé Les valeurs d'infiltration nette, de temps de parcours de l'eau souterraine et de la recharge sont nécessaires sur le site de Yucca Mountain, Nevada, USA, pour évaluer les capacités d'un site de stockage potentiel pour le confinement de déchets hautement radioactifs. Cependant, la complexité géologique du site, les faibles valeurs de précipitation et d'infiltration nette, associées à de nombreux mécanismes agissant simultanément pour faire se déplacer l'eau dans le système, posent de nombreux problèmes pour estimer la distribution spatiale de la recharge. Un ensemble de méthodes adaptées aux environnements arides a été mis en œuvre, comprenant les techniques de bilan hydrologique, des calculs s'appuyant sur la loi de Darcy en milieu non saturé, une méthode de physique des sols appliquée aux données de teneur en eau par mesure neutronique, une modélisation inverse des profils thermiques en forage portant sur l'épaisse zone non saturée, le bilan de masse des chlorures, les radionucléides atmosphériques et des approches empiriques. Ces méthodes indiquent que les taux d'infiltration au voisinage de la surface à Yucca Mountain sont très variables dans le temps et dans l'espace, avec des valeurs locales, ponctuelles, comprises entre 0 et plusieurs centaines de mm/an. Les valeurs d'infiltration nette distribuées dans l'espace sont en moyenne de 5 mm/an, les plus fortes approchant 20 mm/an. Ces résultats ont été introduits dans un modèle à l'échelle du site qui a été calibré au moyen de ces jeux de données, reflétant les processus d'infiltration agissant à des échelles de temps et d'espace à forte variabilité. L'étude par modélisation prédit une recharge fortement non uniforme de la nappe, dont la distribution est significativement différente de l'organisation de l'infiltration non uniforme en surface.

Resumen Se necesitan conocer los valores de infiltración neta, el tiempo de tránsito de las aguas subterráneas y la recarga en el emplazamiento de Yucca Mountain, Nevada, USA, con el fin de evaluar el comportamiento esperado de un repositorio potencial como sistema de contención de residuos de alta radioactividad. Sin embargo, la complejidad geológica del lugar y los pequeños valores de precipitación e infiltración neta, junto con los

Received: 12 May 2001 / Accepted: 12 August 2001
Published online: 11 January 2002

© Springer-Verlag 2002

A.L. Flint (✉) · L.E. Flint
US Geological Survey, Placer Hall, 6000 J Street, Sacramento,
California 95819-6129, USA
e-mail: aflint@usgs.gov
Fax: +1-916-278-3225

E.M. Kwicklis · J.T. Fabryka-Martin
Los Alamos National Laboratory, P.O. Box 1663, Los Alamos,
New Mexico 87545, USA

G.S. Bodvarsson
Lawrence Berkeley National Laboratory, 1 Cyclotron Road,
MS 90-1116, Berkeley, California 94720, USA

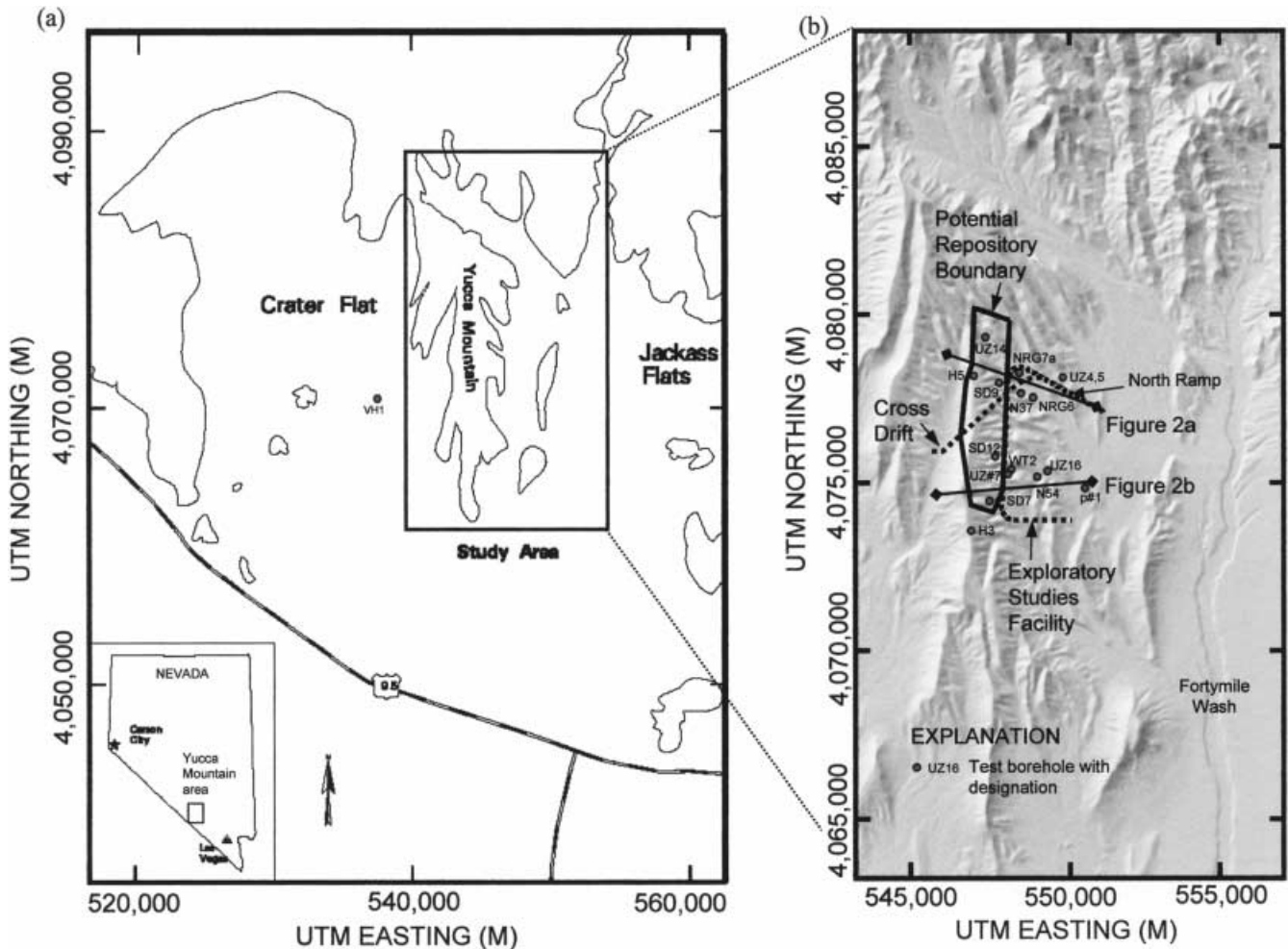


Fig. 1 Location of **a** the Yucca Mountain area, Nevada, and **b** general study area

numerosos mecanismos que operan simultáneamente en relación con el movimiento del agua en el sistema, representan un enorme reto para la estimación de la distribución espacial de la recarga. Se ha aplicado diversos métodos considerados apropiados para medios áridos: técnicas de balance de agua, cálculos basados en la ley de Darcy en la zona no saturada, un método de mecánica de suelos para conocer el contenido de agua con sondas de neutrones en sondeos, modelación inversa de los perfiles de sondeos a lo largo de una zona no saturada gruesa, balance de masas de cloruros, radionucleidos atmosféricos y técnicas ambientales. Estos métodos indican que, cerca de la superficie, las tasas de infiltración en Yucca Mountain son muy variables en el tiempo y el espacio, presentando valores locales (puntuales) comprendidos entre cero y varios cientos de mm/a. Los valores espaciales de la infiltración neta tienen un promedio de 5 mm/a, con máximos cercanos a 20 mm/a. Estos resultados han sido incorporados a un modelo que se ha calibrado con los datos existentes, que reflejan la elevada variabilidad temporal y espacial de los procesos de infiltración. El modelo predice una recarga muy poco uniforme, distribuida

de forma significativamente diferente al esquema no uniforme de infiltración en superficie.

Keywords Groundwater recharge · Infiltration · Unsaturated zone · Arid regions · USA

Introduction

Estimating recharge in the desert southwest of the USA involves a large degree of relative uncertainty due to low precipitation and high evapotranspiration. This task is particularly challenging at Yucca Mountain, Nevada, the potential site of the Nation's first repository for high-level radioactive waste and spent nuclear fuel (Fig. 1). This location was selected because of the thick unsaturated zone, consisting of layers of nonwelded and welded tuffs that are variably fractured and faulted, thereby enhancing drainage in the unsaturated repository horizon. Various scales of studies have been conducted at this site. Some of these are regional in scope and include the area shown in Fig. 1a; most of the modeling and recharge estimates have been made within the boundaries of Fig. 1b. Estimates of net infiltration, groundwater travel time, and recharge are necessary at this site in order to evaluate the expected performance of the potential repository as a waste-isolation system.

This paper summarizes and evaluates recharge-estimation methods applied at Yucca Mountain; each method addresses a different scale and is controlled by different mechanisms and features operating in the unsaturated zone:

1. *Physical methods* solve for liquid flux in heat or moisture-transport equations, for a specified set of hydrologic parameters and bounding conditions. Physical methods applied at Yucca Mountain include Darcian methods applied to saturation or water-potential data from various hydrostratigraphic layers at Yucca Mountain, direct measurement of changes in water content in a network of neutron-access boreholes, and inverse heat-flow models to match temperature profiles in deep boreholes.
2. *Empirical methods* are those using equations that employ a characteristic such as precipitation to spatially distribute a related feature such as recharge. In the desert southwest, where precipitation is the primary limiting factor for recharge, it is a reasonable surrogate for the distribution of recharge if the distribution of precipitation is well characterized.
3. *Environmental-tracer methods* estimate the infiltration rate or age of water at a given depth based on in-situ concentrations of some natural constituent, the concentration of which can be defined by a time-dependent function. Environmental tracers measured at Yucca Mountain include chloride, atmospheric radionuclides (tritium, carbon-14, chlorine-36), and stable isotopes of hydrogen or oxygen.
4. *Watershed modeling* is based on the assumption that net infiltration is the same as recharge on a watershed scale. The watershed model developed for Yucca Mountain uses a water mass-balance approach in which measured or stochastically simulated precipitation, the physical setting, and hydrologic properties of the site approximate the actual conditions at Yucca Mountain.

The last section of this paper addresses how the disparate results from these various recharge-estimation methods, which address both one-dimensional and two-dimensional processes, have been used in process models and in three-dimensional site-scale models to define upper-boundary conditions, to evaluate hydrologic parameter values, and to calibrate and test the models.

Because of many unresolved uncertainties associated with these different methods for estimating infiltration and recharge rates, the authors of this paper and their colleagues continue to evaluate the interpretations and applicability of each approach. Rather than striving for complete consensus, however, as many of the methods are included as is practical, regardless of whether or not agreement has been reached on the robustness of a particular data set or the applicability of a particular method for estimation of recharge at Yucca Mountain. The appropriate application of each method is determined by the scale of investigation, the mechanism sought for un-

derstanding, availability of data of adequate quantity and quality, and the spatial and temporal resolution of the results.

Definitions of Terms

Any comparison of recharge estimation methods must recognize the distinctions among the various terms used to refer to water movement in the subsurface. *Percolation flux* applies to the volumetric rate of water movement per unit area at a particular depth. Near the surface, this term is synonymous with *net infiltration*, which is defined as the percolation flux that passes the depth below which the rate of water removal by evapotranspiration becomes insignificant. Net infiltration commonly defines the upper boundary condition for hydrologic models of the unsaturated zone. At increasing depths, however, the magnitude of the percolation flux at a particular point often differs from that of the net infiltration directly above, because water is redistributed in response to changes in the hydrologic properties of rocks and structural features. A knowledge of the percolation-flux magnitude, its spatial and temporal variability, and mode of delivery as fracture- or matrix-derived flow at the depth of the potential repository is important to ensure a suitable engineering design of the waste-containment system at the site, and to understand the relevance of the numerous mechanisms and features that influence the movement and distribution of water through the deep unsaturated zone. *Recharge* is the volumetric rate of water crossing the water table and entering the groundwater flow system. This term defines the upper boundary condition for saturated-zone models used to calculate travel time from beneath Yucca Mountain to the accessible environment.

Under steady-state conditions, net infiltration at the surface becomes recharge to the water table except when perched water discharges at springs and is lost to evapotranspiration (which is not an issue at Yucca Mountain under its present-day climate). The rate of net infiltration, unsaturated-zone thickness, and effective flow-pathway porosity control travel time through the unsaturated zone (Flint et al. 2000). Net infiltration – and, therefore, recharge – varies spatially due to variations in surface microclimates, alluvial thickness, faults and fractures, and thickness and hydrologic properties of geologic strata in the unsaturated zone. To some extent, temporal fluctuations in surface infiltration are expected to be damped with depth, but recharge is nonetheless expected to vary on time scales of centuries to millennia (Flint et al. 2000).

The methods described in this paper yield results that represent these different temporal and spatial scales. Consequently, two methods applied to today's measured data may yield different fluxes, yet both could be correct. For example, neutron-hole moisture data used to calculate near-surface fluxes over the last 15 years may correctly represent average conditions over that period of

time, yet be in apparent disagreement with fluxes estimated by applying the chloride mass-balance method to pore waters extracted from drill core, because the latter method may be representing fluxes that were in effect hundreds or even thousands of years ago. Recharge-estimation methods based on deeper measurements presumably integrate, or average out, the excursions caused by local, near-surface processes. Considerable additional complexity to the system also results from the fact that the relative proportions of matrix and fracture flow are expected to change with time and with depth in response to changes in climate and the resulting percolation fluxes, and due to contrasts in hydraulic conductivities and fracture geometries in the different stratigraphic units.

Yucca Mountain Site Description

Yucca Mountain is located in southern Nevada, about 160 km northwest of Las Vegas (Fig. 1). The general study area (Fig. 1b) covers approximately 60 km², of which 5 km² is the potential repository site, the site proposed for the storage of high-level radioactive waste. Beneath the crest of Yucca Mountain, the water-table depth is approximately 350–750 m below land surface and averages 500 m. The potential repository horizon is in the unsaturated zone at an average depth of 300 m below land surface, within the Topopah Spring Tuff of the Paintbrush Group, a densely welded and fractured tuff (Fig. 2). Site characterization has been ongoing since the late 1970s. On-site investigations have consisted primarily of studies of surface processes and site characterization; surface-based boreholes that penetrate to various depths, ranging from shallow depths to below the water table; an underground Exploratory Studies Facility (ESF; Figs. 1b and 2), 8 km in length, that extends from the ground surface to the depth of the potential repository; and a Cross Drift that extends 2.5 km across the potential repository within the repository horizon (Figs. 1b and 2).

The unsaturated zone at Yucca Mountain consists of a sequence of ash-flow and ash-fall tuffs, 550–750 m thick (Buesch et al. 1996). From youngest to oldest, the formations in the unsaturated zone are the Tiva Canyon (TCw), Yucca Mountain, Pah Canyon, and Topopah Spring (Tpt) Tuffs of the Paintbrush Group; the Calico Hills Formation (Tac); and the Prow Pass Tuff (Tep) of the Crater Flat Group (Fig. 2). Interstratified with these formations are bedded tuffs that consist primarily of fallout tephra deposits and small amounts of pyroclastic flow deposits and reworked material (Buesch et al. 1996). The bottom and top of the Tiva Canyon and Topopah Spring Tuffs contain nonwelded to densely welded tuff, and the interiors of the tuffs are thick, moderately to densely welded, and fractured. The Yucca Mountain and Pah Canyon Tuffs contain both nonwelded and welded intervals. The nonwelded tuffs of the Paintbrush Group, including the nonwelded intervals of the Yucca Mountain and Pah Canyon Tuffs, the interstratified bedded tuffs, the nonwelded base of the Tiva Can-

yon Tuff, and the nonwelded top of the Topopah Spring Tuff, collectively are commonly referred to as the Paintbrush nonwelded hydrogeologic unit (PTn). The Calico Hills Formation (Tac) is composed of nonwelded pyroclastic flow and fallout deposits. The Prow Pass Tuff consists of nonwelded to partially welded rocks at the top and bottom, with intervals of welded tuff.

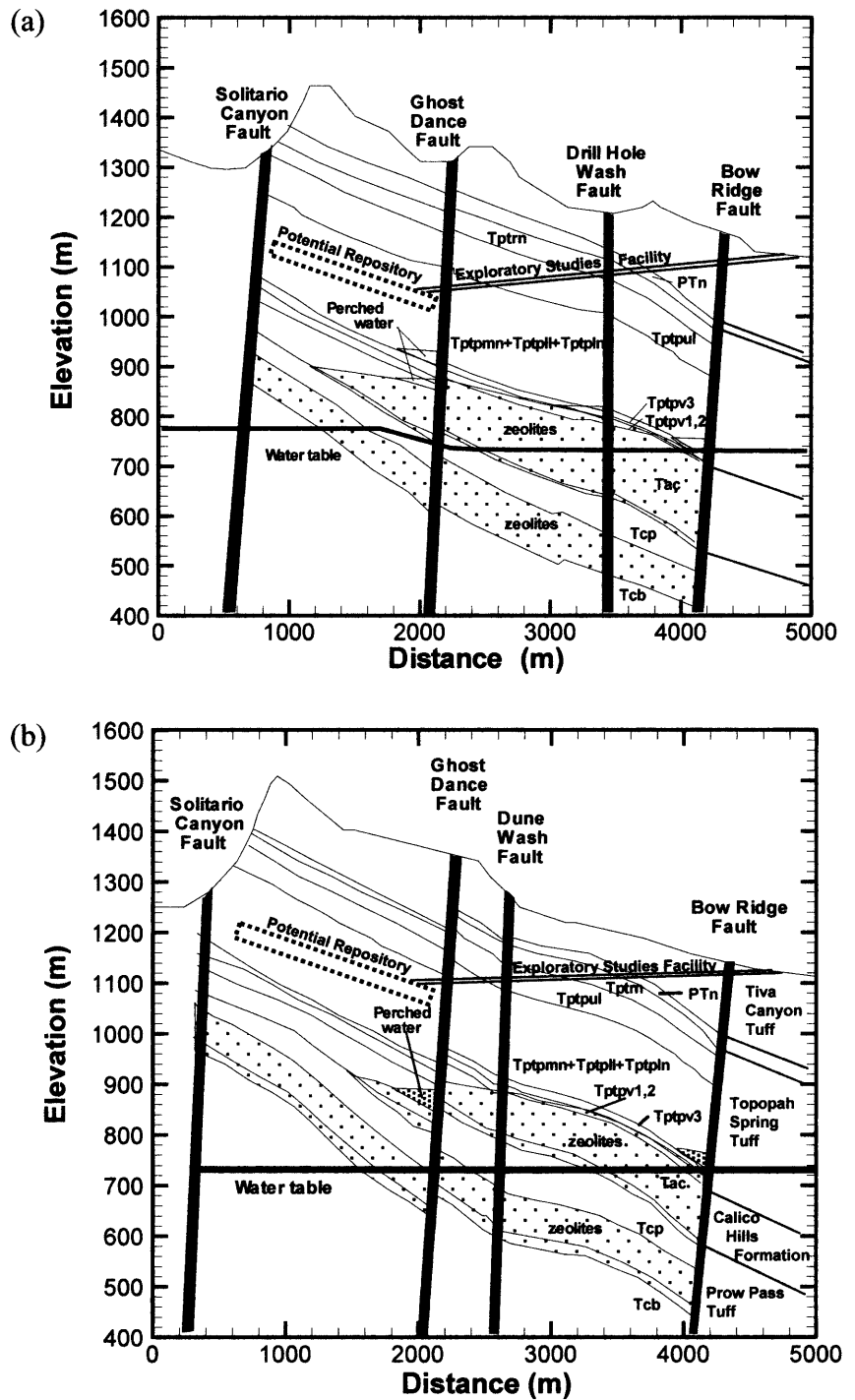
Methods for Estimating Recharge at Yucca Mountain

Darcian Methods

Methods based on the application of Darcy's law use estimates of the measured or estimated effective hydraulic conductivity of the rock at its prevailing state of water potential or saturation, in combination with estimates of the hydraulic-head gradient, to directly calculate percolation flux using Darcy's law. In the absence of detailed head measurements to calculate the gradient, it is assumed that a unit gradient exists at some depth below the surface. This method is also the basis for estimates of percolation flux that is produced from model calibration, using existing borehole saturation and water-potential data sets. In this approach, percolation flux is adjusted until an optimal match between the observed data and the model output is achieved (Ahlers et al. 1995; Bodvarsson and Bandurraga 1996). Flux estimates by Darcian methods are more likely to be reliable in cases for which it can reasonably be assumed that most of the flow of water is through the rock matrix rather than through fractures. At Yucca Mountain, this assumption may be met with more confidence in the nonwelded vitric tuffs, such as the Paintbrush nonwelded hydrogeologic unit (PTn; Fig. 2), where fractures are generally relatively sparse, intrinsic matrix permeabilities are relatively high, and the rocks are unsaturated. Darcian methods are subject to uncertainty in the relation between unsaturated hydraulic conductivity and saturation (or water potential), particularly at low saturations, where difficulty in obtaining direct measurements of effective hydraulic conductivity often lends greater uncertainty to the flux estimate.

Two Darcian approaches have been used to estimate percolation flux from saturation and water-potential data at Yucca Mountain. In one approach, numerical models that embody Darcy's law through the Richards equation or its multiphase equivalent are used to calculate saturations and water potentials for different assumed flux values, given the measured or estimated rock-matrix hydraulic properties of different hydrostratigraphic layers. Percolation fluxes are estimated by minimizing the differences in the measured and simulated water saturations and water potentials, either by a trial-and-error approach (for example, see Kwicklis et al. 1994) or through automated parameter-estimation methods (for example, see Bandurraga et al. 1996; their approach is also summarized in Bandurraga and Bodvarsson 1999). Parameter-estimation methods have an advantage over trial-and-error

Fig. 2a,b Geologic sections of the Yucca Mountain site, indicating dominant features and processes. Sections are located **a** in the north, and **b** in the south. Lines of sections are shown in Fig. 1b. Lithostratigraphic abbreviations are from Buesch et al. (1996). Vertical axis is exaggerated 4X



ror methods in that the former can provide quantitative measures of uncertainty in the estimated parameters. The second approach estimates flux directly from Darcy's law, by using field measurements of saturation or water potential with measured or estimated functional relations between effective hydraulic conductivity and the variables measured in the field (for example, see Weeks and Wilson 1984). Kwicklis et al. (1993) also applied this method to data collected from two boreholes at Yucca Mountain. Borehole UZ#4 is located in an active channel,

and borehole UZ#5 is located 35 m away on the side slope of the wash (Fig. 1). At these boreholes, nearly continuous profiles of percolation flux were estimated for the tuff units using measured saturation and porosity data from the boreholes (Loskot and Hammermeister 1992). Correlations between saturated and unsaturated hydraulic parameters and porosity were derived from data in Peters et al. (1984). Porosity data from UZ#4 and UZ#5 and the hydraulic-property correlations formed the basis for assigning hydraulic properties to various depth intervals in the boreholes.

An advantage of using a direct Darcy's law approach is that these direct calculations of flux do not require the assumption of steady state or of strictly vertical flow if local gradients are known. Calculations for boreholes UZ#4 and UZ#5 (Kwicklis et al. 1993, Fig. 13) indicate fluxes larger than 1 m/year at the shallowest depths for which data were available (25–30 m) and fluxes less than 1 mm/year deeper in the boreholes, suggesting that a relatively large pulse of water had recently entered the system and that a significant portion of it had been either laterally diverted or converted to fracture flow. Additionally, systematic changes in the estimated flux with depth at both boreholes suggest that lateral flow along bedded tuff subunits within the PTn had occurred.

Estimates of flux are also being calculated for two boreholes vertically penetrating the PTn and the upper rocks of the welded Topopah Spring Tuff in alcoves 770 m apart along the north ramp of the ESF (Fig. 1b). Calculations are based on in-situ water-potential measurements from heat-dissipation probes installed in the boreholes, and on hydraulic properties measured directly on samples taken from similar locations within each hydrostratigraphic unit exposed along the north ramp. The first 5–14 m of the boreholes show the effects of evaporation due to ventilation in the drift. Away from this influence, flux is downward in the boreholes at rates of approximately 8–15 mm/year in the nonwelded PTn, and approximately 1 mm/year in the underlying Topopah Spring Tuff densely welded rocks. Once again, these flux estimates suggest that a significant portion of the flux through the PTn is either laterally diverted or converted to fracture flow when it reaches the more welded unit below. Calculations of flux along the 6.5-degree slope between the two boreholes result in less than 1 mm/year down-dip flux in either the base of the PTn or in the welded top of the Topopah Spring Tuff, supporting the suggestion that water is converted to fracture flow once it penetrates the welded rocks. However, because estimated or measured hydraulic conductivities for samples with low saturations have large uncertainties, the calculated fluxes are accurate only within an order of magnitude. The Darcy's law approach, although often providing an enhanced understanding of the local mechanisms contributing to subsurface water flow, can only provide bounding estimates of flux in the unsaturated zone at Yucca Mountain.

Neutron Logging of Moisture Profiles

Volumetric water content was measured in neutron-access boreholes using neutron moisture meters for 12 years in about 99 boreholes representing four topographic zones: channel, terrace, side slope, and ridge top (Flint and Flint 1995, 2000). Net infiltration was estimated by determining the increase in the water content below the zone of evapotranspiration, which is assumed to be 2 m below the soil–bedrock interface if the soil is thinner than 6 m, or 6 m into the soil for deeper soils. The sum of increases in volumetric water content for a

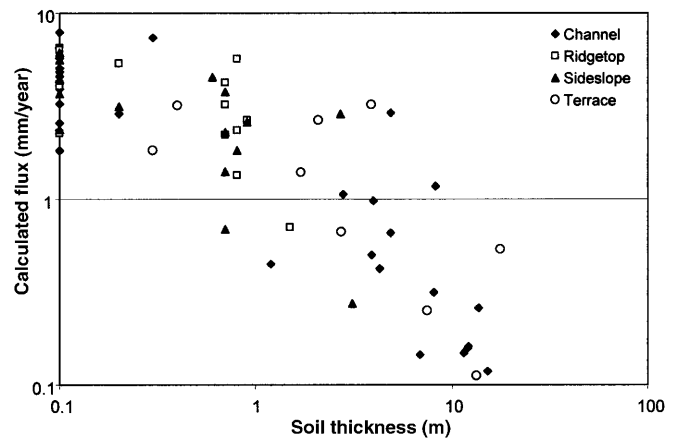


Fig. 3 Flux calculated for 80 neutron-access boreholes compared to soil thickness at each borehole for four types of geomorphologic settings

depth interval multiplied by the length of this interval (McElroy 1993) is a minimum (conservative) estimate of net infiltration, because fracture flow that bypasses the surrounding rock matrix is not included in the measurement. Shallow fractures at this site are often filled with carbonate materials; thus this omission is not considered significant, particularly on a volumetric basis. The increase in volumetric water content for the depth interval in the borehole from 2 m below the soil–bedrock interface to total depth, multiplied by that depth, as a function of the time interval, is flux, in millimeters per year.

Using calculations of flux for all boreholes and regression analysis, it was determined that five factors significantly affected net infiltration: precipitation, soil thickness, bedrock geology, geomorphologic location, and aspect (Flint et al. 2001a). The values of flux affected by geomorphic location and soil thickness are presented in Fig. 3. This figure shows that the soil thickness influences net infiltration. It also shows that for the suite of 80 boreholes for which flux was calculated (some holes were considered unsuitable for evaluation due to apparent leakage down the casing), only four channel boreholes with more than 2 m of soil cover showed a measurable amount of flux, greater than 0.9 mm/year. These four boreholes are located in washes that received several runoff events during the period of monitoring. Channels located in the heads of drainages, where there was no soil cover, showed substantial fluxes. The average total volume of net infiltration, in cubic meters, contributed by the various geomorphologic locations per year is calculated as the average flux for the boreholes from each location in Fig. 3, in millimeters per year, multiplied by the area within the site occupied by those locations, as well as the percentage of the total flux for the site per year. The percent of total net infiltration volumes for the geomorphologic locations are: ridge top, 19%; side slope, 73%; terrace, 7%; and channel, 1%. This result indicates that the side slope contributes a far greater volume of net infiltration than the other geomor-

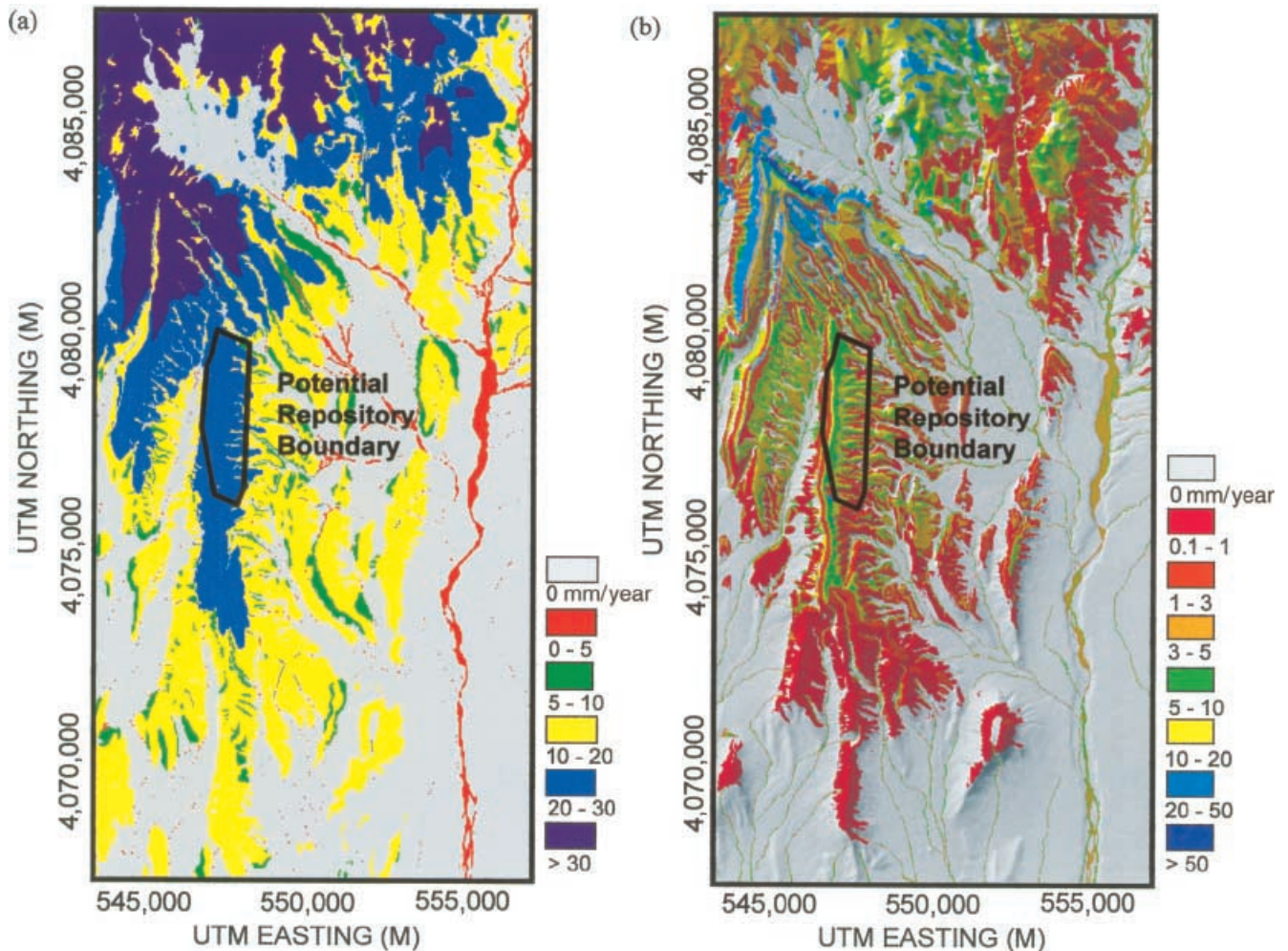


Fig. 4 Spatially-distributed net infiltration at Yucca Mountain using **a** statistical analyses (from Flint et al. 2001a) and **b** numerical modeling (from Flint et al. 2001b)

phologic locations, because of the rapid surface infiltration and large percentage of the total area. The channels, despite the large volumes of water available from concentrated runoff, contribute less, at least under the present dry climate.

Flint et al. (2001b) used neutron moisture logs recorded in 69 boreholes over 11 years to develop estimates of shallow infiltration at Yucca Mountain (Fig. 4a); these estimates served as the basis for developing a numerical infiltration model (Fig. 4b, discussed later, under Watershed Modeling). At the boreholes from which the moisture logs were obtained, a correlation was established between (1) shallow infiltration and precipitation, and (2) depth of alluvial cover. Net infiltration at individual boreholes was estimated from the neutron logs to be the changes in moisture content that occurred below a 2-m depth in bedrock. Shallow infiltration in areas between the boreholes was determined from the correlation and estimates of the distribution of soil thickness and precipitation. The calculated average shallow infiltration for the entire modeled area is 11.6 mm/year; upland areas in

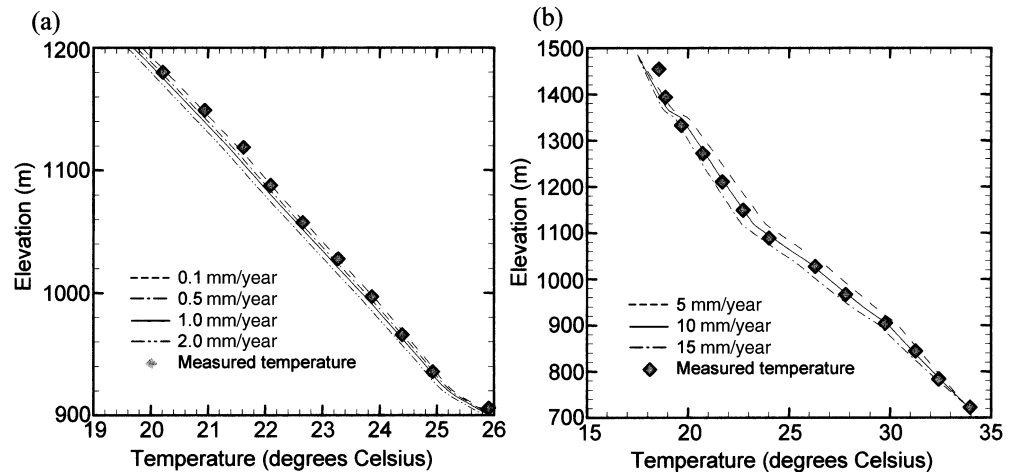
the central block of Yucca Mountain receive 20–30 mm/year and the lower elevation areas in the central block generally receive 10–20 mm/year. Although this method provides point information, statistically correlated surface features, including precipitation, were used to estimate fluxes between boreholes.

One of the limitations in using this method is that it cannot detect steady-state components of recharge. The method is good for identifying changes in storage as one component of the water mass-balance equation for estimating shallow infiltration, which is its application in this particular case. In arid environments, where fluxes in the near surface are sporadic, often occurring only once every few years, the potential for steady-state downward flux in the shallow surface is unlikely to be a significant issue. However, fluxes that occur without causing a change in storage (such as fracture flow, or deep percolation under quasi-steady state conditions in the unsaturated zone) remain undetected by this method.

Borehole Temperature Profiles

Because water consumes heat as it moves from cooler, shallow depths to warmer, deeper environments, borehole temperature profiles are potentially sensitive indica-

Fig. 5 Temperature profiles modeled using various fluxes for boreholes **a** WT-2 and **b** H-3. Temperature data are from Sass et al. (1988). Borehole locations are shown in Fig. 1b



tors of the percolation flux. The deviation of a measured temperature profile from a heat-conduction-only profile is used to estimate percolation flux. This method has several advantages over other methods, including the sensitivity of temperature to mass flux rather than velocity, the potential for temperature to reflect the matrix and fracture components of the flux, and the relative insensitivity of thermal conductivity to variations in saturation and water potential, as compared to highly sensitive hydraulic parameters such as hydraulic conductivity. This approach also integrates many features, providing a borehole-scale estimate of flux.

In the present study, percolation fluxes were estimated for a subset of the boreholes using TOUGH2 (Pruess 1991). Boreholes selected for analysis were chosen on the basis of data density, apparent data quality, and geographic distribution. The temperature profile for each borehole (Sass et al. 1988) was simulated numerically, and the assumed percolation flux for the model at each borehole was varied to visually optimize the fit between the measured and simulated profiles (Fig. 5). Average annual ground-surface temperatures estimated for individual boreholes and measured temperature of the groundwater in the upper part of the saturated zone formed the upper and lower boundary conditions for the models.

The temperature-profile data set of Sass et al. (1988) was one of the earliest data sets used to indicate that the percolation flux at Yucca Mountain is significantly higher than the submillimeter per year range. The percolation fluxes obtained by optimizing the match between the measured and simulated temperature profiles at ten deep boreholes from various topographic locations range in flux from 0.5–20 mm/year, with the highest flux being determined for H-5 on the crest of Yucca Mountain. Simulation results for two of these boreholes are shown in Fig. 5. The goodness-of-fit and sensitivity of the simulated temperature profiles to changes in the percolation fluxes are evident in this figure. In most cases, the fit is good and the flux is reasonably well constrained by the data within an order of magnitude.

A similar analysis of percolation flux was conducted for boreholes UZ#4 and UZ#5, which are located in an alluvial channel and bedrock side slope, respectively, about 2 km north of the ESF. This analysis used temperature measurements (Kwicklis 1999) that indicate long-term fluxes of 18 mm/year at UZ#4, and 5 mm/year at UZ#5. These boreholes are only 35 m apart but have distinctly different temperature profiles. Although the measured temperature values in each borehole are certainly influenced by a surrounding volume of rock that is larger than the borehole itself, the size of this effective rock volume cannot be determined on the basis of available data.

Empirical Methods

Maxey and Eakin (1950) developed an empirical method to estimate recharge to groundwater basins in Nevada, providing a baseline for the spatial distribution of recharge on a subbasin scale. This method uses average annual precipitation to classify areas of a basin into five recharge zones. Each zone uses a different percentage of average annual precipitation becoming recharge: 0% recharge for less than 203 mm/year average annual precipitation, 3% for 203–304 mm/year, 7% for 305–380 mm/year, 15% for 381–507 mm/year, and 25% for 508 mm/year or greater.

The results of several studies were incorporated by Hevesi and Flint (1998) into the development of a modified Maxey-Eakin model for estimating recharge on a regional scale and for providing a general estimate of site-scale recharge at Yucca Mountain. This model was a fit through the original step function developed by Maxey and Eakin (1950) with a lower limit of recharge set to average annual precipitation of 100 mm, instead of the 203 mm/year lower limit for recharge used by Maxey and Eakin. Using an estimate of regional precipitation (average annual precipitation of 175 mm/year) and the modified model, recharge was estimated to be 2.9 mm/year for the Death Valley region and 0.2–1.4 mm/year at Yucca Mountain. The original Maxey-Eakin

model yielded an estimate of zero recharge. The basins used by Maxey and Eakin (1950) to develop their model were dominated by alluvial fill, in contrast to Yucca Mountain, which is dominated by upland areas with thin soils, thus warranting the modification to the model. This, and the difficulty extrapolating the original model at the dry end, are possible explanations for the low estimates when the Maxey-Eakin model is applied to Yucca Mountain. In addition, the Maxey-Eakin methods only consider precipitation; therefore the shallow soil depth and high bedrock permeability that tend to enhance net infiltration at Yucca Mountain are not incorporated.

Chloride Mass-Balance Method

The chloride mass-balance (CMB) approach is based on the premise that the flux of chloride (Cl) deposited at the surface equals the flux of Cl carried beneath the root zone by infiltrating water. With increasing depth, as water is extracted by evapotranspiration, Cl concentrations in pore waters increase and apparent infiltration rates decrease. Net infiltration is the flux of water moving below the zone of evapotranspiration, such that Cl concentrations remain relatively constant below this depth. Net infiltration rates can thus be estimated from measured Cl concentrations using the relationship:

$$I = (P C_0) / C_s \quad (1)$$

where I is average net infiltration (mm/year); P is average annual precipitation (mm/year); C_0 is the effective average Cl concentration in precipitation (mg/L), including the contribution from dry fallout; and C_s is the measured Cl concentration in subsurface water (mg/L), which can be pore water, perched water, or groundwater.

This approach has been widely used to estimate water-transport rates in alluvial profiles through the unsaturated zone as well as basin-wide recharge (for example, see Dettinger 1989; Phillips 1994; Lichty and McKinley 1995; Scanlon et al. 1997). Parameter values adopted for application of the CMB method at Yucca Mountain are an average annual precipitation rate of 170 mm/year and an average Cl concentration of 0.35 mg/L, based on a review of regional bulk precipitation data and the background $^{36}\text{Cl}/\text{Cl}$ ratio for this site and assuming that the total annual Cl deposition rate (the product $P C_0$) is constant over time (section 3.9.2.3 in CRWMS M&O 2000a). Cl concentrations of 0.3 mg/L reported by Hershey (1989) for high-altitude springs in the Spring Mountain Range, which lies between Yucca Mountain and Las Vegas, support the adopted value.

Applicability of the CMB method to the specific conditions at Yucca Mountain (for example, shallow soil cover over fractured rock) could violate some of the underlying assumptions for this method. For example, relatively dilute water that has infiltrated rapidly through fracture pathways may be inadequately represented by matrix pore water because of incomplete mixing, in which case matrix pore-water samples might be biased

toward the slower-moving, more concentrated matrix component of flow. Percolation estimates based on these samples would constitute lower bounds on the actual percolation rates. A distinct Cl bulge occurs in the uppermost 5 m of all soil profiles, as has been widely observed in soil profiles at other arid sites (for example, see Phillips 1994), but the implications of this bulge for interpreting Cl concentrations in terms of infiltration rates have not been evaluated conclusively. In addition, although substantial runoff/run on does not occur often at Yucca Mountain, sometimes runoff concentrates in washes or flows laterally along the alluvium/bedrock interface at the base of side slopes. Because runoff has higher total Cl concentration (typically about 3 mg/L; Fabryka-Martin et al. 1997) than that in precipitation, rough calculations suggest that this mechanism could lead to underestimates of infiltration beneath channels by an order of magnitude, even assuming that only 1% of the precipitation in a watershed reaches the channel. Despite these unresolved questions, however, the method appears to be valid for a first approximation of infiltration at Yucca Mountain, as judged by its consistency with most other data sets discussed in this paper.

Pore waters

Pore-water Cl concentrations at Yucca Mountain are highly variable, ranging from 6–245 mg/L in the tuff matrix, and as much as several thousand mg/L in deep alluvium (Yang et al. 1996, 1998; Tables 6, 26, and 27 in CRWMS M&O 2000a). Corresponding values of net infiltration estimated by the CMB method range from less than 0.1 to 10 mm/year for a variety of topographic settings. Table 1 summarizes Cl pore-water concentrations for selected samples from boreholes drilled at the surface of Yucca Mountain and underground in the ESF. Concentrations in the PTn matrix are vertically heterogeneous; often concentrations are higher near the top of the unit than lower in the profile. The concentrations cited in Table 1 are the lowest values measured in the indicated stratigraphic unit for each location, under the assumption that these represent well-mixed pore waters from active flow paths. However, they could also reflect dilution with water transported laterally from adjacent higher-infiltration zones. These data, along with supporting information from neutron-moisture logging and ^{36}Cl and tritium analyses, indicate that thick alluvium is generally an effective barrier to water movement, and the data confirm that infiltration is indeed higher where alluvial cover is thin or absent. Apparent infiltration rates are <1 mm/year beneath thick alluvium in large washes, channels, or terraces, and somewhat higher (1–2 mm/year) for samples from the PTn below these topographic settings, possibly due to lateral flow entering the channel along the bedrock/alluvial contact at the base of side slopes. The highest infiltration rates (4–10 mm/year) occur beneath areas with negligible soil cover, such as ridge tops and side slopes that typify the topography above the Cross Drift and the ESF.

Table 1 Apparent infiltration rates calculated from representative pore-water chloride concentrations at Yucca Mountain

Borehole location	Chloride concentration ^a (mg/L)	Apparent infiltration rate ^b (mm/year)
Alluvial sample from depths greater than 5 m (large washes and thick terraces)		
UZ-N37	133	0.4
UZ-N54	7,400	0.01
UZ-14	520	0.1
UZ#16	3,700	0.02
Sample from PTn beneath area with thick alluvial cover (large washes and thick terraces)		
UZ#4	104	0.6
UZ#5	42	1.4
UZ-14	44	1.4
UZ#16	32	1.8
NRG-6	47	1.3
SD-9	40	1.5
Sample from PTn beneath area with moderate alluvial cover (terrace or near base of sideslope, soil 0.5–3 m)		
NRG-7a	39	1.5
SD-12	46	1.3
UZ-7a	60	1.0
Sample from PTn or TSw beneath area with thin alluvial cover (ridgetop or sideslope, soil <0.5 m thick)		
SD-6 (PTn)	27	2.2
SD-7 (PTn)	77	0.8
UZ-N55 (PTn)	77	0.8
ESF North Ramp (PTn)	6	9.9
ESF South Ramp (PTn)	17	3.5
ESF Main Drift (TSw)	16	3.7
Cross Drift (TSw)	12	5.0

^a Cl concentrations for alluvial samples are averages for depths >5 m in order to ensure that they reflect concentrations below the zone of evapotranspiration. Concentrations cited for pore-water samples from PTn and TSw units are the lowest values of those measured in those stratigraphic units at each location. Data are from Tables 6, 26, and 27 in CRWMS M&O (2000a)

^b Infiltration-rate calculation assumes an average annual precipitation of 170 mm (Hevesi et al. 1992), with an average chloride concentration of 0.35 mg/L (CRWMS M&O 2000a)

Perched waters

Pore-water Cl concentrations provide essentially point estimates of infiltration rates that are useful for evaluating spatial variations in infiltration but are subject to the problems of a spatially biased sampling network and large variability in concentrations even among adjacent samples. Cl concentrations of perched waters and groundwaters potentially are more representative of net infiltration over a larger area and are likely to reflect the flux-weighted contributions of water that has moved through both the rock matrix and along fractures and faults. Perched water occurs at several locations at depths of several hundred meters in the unsaturated zone at Yucca Mountain (O'Brien 1997; Patterson 1999). General chemical and isotopic characteristics of the perched waters are described in Yang et al. (1996, 1998), and ³⁶Cl/Cl ratios for these waters are reported in Fabryka-Martin et al. (1997, Table 4-16).

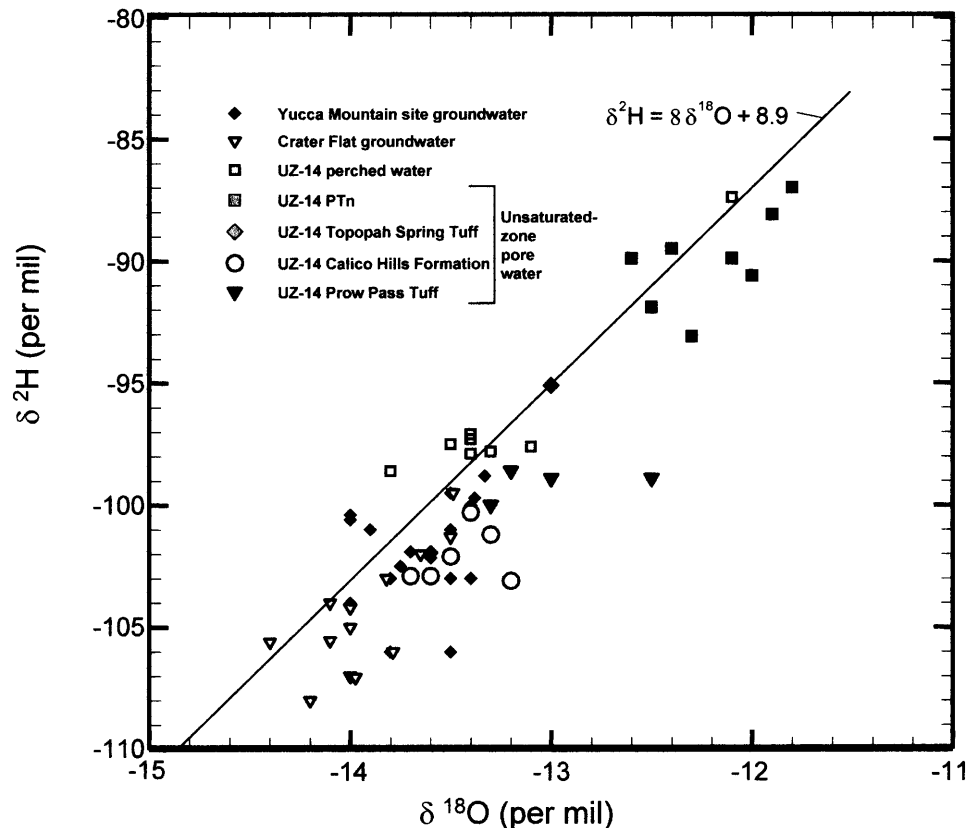
Cl concentrations in perched water are also used to estimate an average infiltration rate. Perched-water concentrations range from 4–7 mg/L, implying local infiltration rates in the order of 8–15 mm/year. In general, Cl concentrations from pore waters and perched water in the deep unsaturated zone are significantly lower than Cl concentrations in pore waters from the shallow unsaturated zone. One explanation for this difference is that the Cl data may be biased, because pore-water samples are not available from areas with high net infiltration. These areas are steep side slopes, where drill rigs cannot be set

up. Secondly, water in the lower unsaturated zone is expected to include a large component of Pleistocene water that infiltrated under a wetter climate with more dilute Cl concentrations than at present. The validity of these two hypotheses is supported by results obtained by Sonnenthal and Bodvarsson (1999), who simulated the Cl distribution in the unsaturated zone using a spatially and temporally variable Cl source term at the ground surface that reflected the expected infiltration pattern during the Pleistocene Epoch and under the present-day climate. They achieved good qualitative agreement between the model results and the observed Cl concentration values.

Groundwater

Cl concentrations in groundwater underlying Yucca Mountain provide a basis for estimating the local recharge rate. The typical groundwater concentration of 7 mg/L (Benson and McKinley 1985) implies a local infiltration rate of 8.5 mm/year, corresponding to 5% of the annual precipitation under today's climate. However, the validity of this interpretation is complicated by the likelihood that at least part of the water originated from Pleistocene precipitation, as well as by the possibility that part of the groundwater originated from upgradient sources. The following two sections describe how these complicating factors have been addressed at Yucca Mountain to provide estimates of local recharge under present and past climates.

Fig. 6 $\delta^2\text{H}$ and $\delta^{18}\text{O}$ for unsaturated-zone pore water and perched water from UZ-14, and saturated-zone water from the Yucca Mountain area. Local meteoric water line is from Benson and Klieforth (1989); unsaturated-zone data are from Yang et al. (1996, 1998); groundwater data are from Benson and McKinley (1985) and CRWMS M&O (2000b)



Evidence for Pleistocene water

Consistently lower Cl concentrations observed in water samples from deep locations in the unsaturated zone as compared to shallower locations may in part reflect a temporal shift in infiltration rates related to climate change. In this scenario, the more dilute Cl concentrations represent higher infiltration rates during the wetter, cooler climate of the late Pleistocene Epoch. This view is supported by $\delta^2\text{H}$ and $\delta^{18}\text{O}$ data from the Yucca Mountain area. The $\delta^2\text{H}$ and $\delta^{18}\text{O}$ values of pore water obtained from the unsaturated zone at UZ-14 by compression of core samples (Yang et al. 1998) are shown in Fig. 6. Also shown are data for the perched-water samples from borehole UZ-14, at the northern edge of the ESF; saturated-zone groundwater from boreholes in the Yucca Mountain area and Crater Flat; and the local meteoric water line determined by Benson and Klieforth (1989) from snow samples obtained on Yucca Mountain.

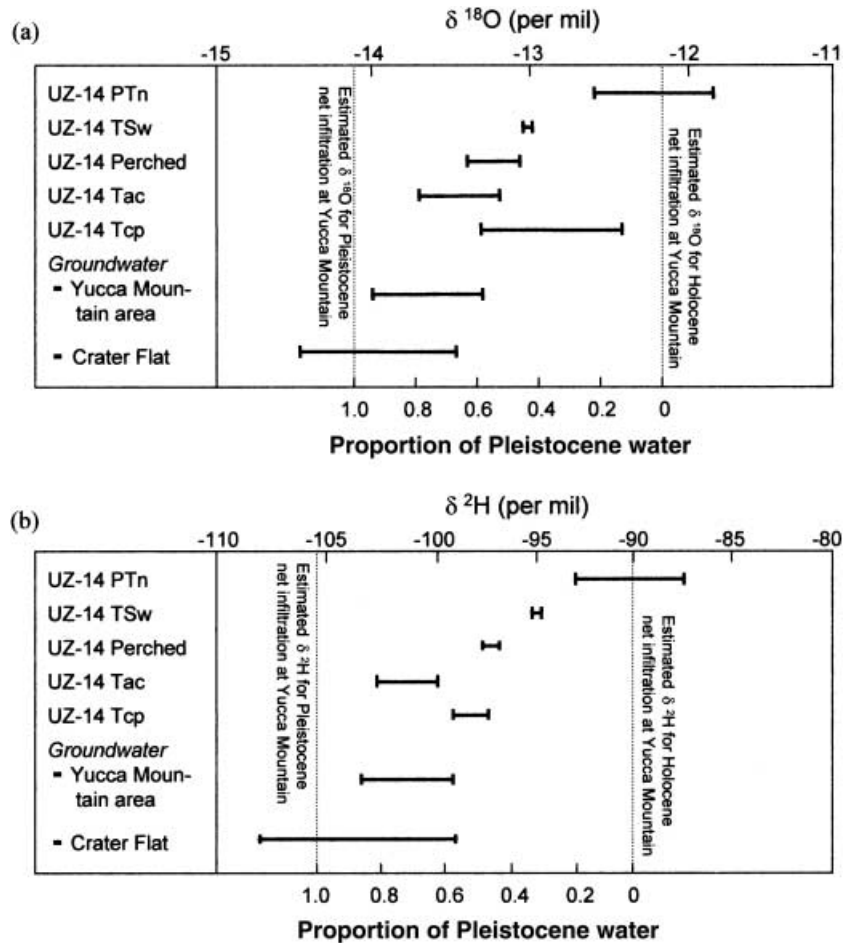
The fraction of Pleistocene water in a given unsaturated-zone formation is estimated from the average $\delta^2\text{H}$ and $\delta^{18}\text{O}$ values of pore waters in a given stratigraphic interval, using a simple two-component mixing model with Holocene and Pleistocene end-members. A significant difference in $\delta^2\text{H}$ and $\delta^{18}\text{O}$ in waters infiltrating during glacial and interglacial periods is expected due to changes in the isotopic signature of the marine source and from the tendency for precipitation to become isotopically lighter with decreasing condensation temperature (Benson and Klieforth 1989). The $\delta^{18}\text{O}$ values for uranium-series-dated samples from a 140-mm-thick calcite

vein in Devil's Hole, located about 75 km southeast of Yucca Mountain, provide a long-term record of climatic variability in the south-central Great Basin (Winograd et al. 1988, 1992). Based on this record, the $\delta^{18}\text{O}$ values of waters that became net infiltration during glacial maxima average about 1.9 per mil lighter than the $\delta^{18}\text{O}$ of water that infiltrated during interglacial periods.

Additional assumptions of this analysis are that (1) infiltrating waters at Yucca Mountain experienced the same total range in $\delta^{18}\text{O}$ values as are observed in Devil's Hole calcite (1.9 per mil); and (2) pore water in the PTn in borehole UZ-14 is representative of the Holocene end-member, based on the relatively shallow depth of this unit and the match with the $\delta^{18}\text{O}$ value predicted for present-day precipitation at the borehole elevation (Ingraham et al. 1991). Ranges of isotopic values measured for pore waters and perched water at UZ-14 are shown in Fig. 7, along with proportions of Pleistocene water estimated using the two-component mixing model. The approach used for $\delta^{18}\text{O}$ data is also applied to $\delta^2\text{H}$ data in Fig. 7, assuming that the $\delta^2\text{H}$ value of infiltrating Pleistocene waters was heavier than Holocene infiltration by 15.2 per mil, calculated from the slope of the local meteoric water line and the adopted range of $\delta^{18}\text{O}$ data (1.9 per mil).

Both isotopes plotted in Fig. 7 show an increasing Pleistocene component in the pore water with increasing stratigraphic depth as water percolates from the PTn through the Topopah Spring Tuff, the perched-water layer, and the Calico Hills Formation. The estimated per-

Fig. 7 Calculated proportions of Pleistocene water, based on **a** $\delta^{18}\text{O}$ and **b** $\delta^2\text{H}$ values of pore-water and perched-water samples from borehole UZ-14, and groundwater samples from the Yucca Mountain area and adjacent Crater Flat. Data sources are the same as for Fig. 6



centage of Pleistocene water in the perched-water layer at UZ-14 is 47 and 50%, based on the measured $\delta^{18}\text{O}$ and $\delta^2\text{H}$ values, respectively. Similarly, $\delta^{18}\text{O}$ and $\delta^2\text{H}$ data for perched water at SD-7 (Yang et al. 1996) indicate that an estimated 58 and 51% of these fluids, respectively, is Pleistocene in origin, consistent with their uncorrected ^{14}C age, which is about 10,500 years for UZ-14 and SD-7. Deeper in the UZ-14 profile, however, the estimated Pleistocene component is significantly greater in the Calico Hills Formation (Tac, about 65%) than in the underlying Prow Pass Tuff (Tcp, about 35%; Fig. 7). Possibly, residual Pleistocene water is more difficult to flush out of the matrix of the Calico Hills Formation due to the extremely low permeability of these zeolitic rocks (Flint 1998, Table 7).

The overall average infiltration rate calculated for the perched waters at Yucca Mountain using the CMB method is deconvoluted into average infiltration rates for the Holocene Epoch and for the Pleistocene Epoch by considering the $^{36}\text{Cl}/\text{Cl}$ and stable Cl data, together with the proportions of Holocene (f^H) and Pleistocene (f^P) components in the perched water, as estimated by using the $\delta^2\text{H}$ or $\delta^{18}\text{O}$ data. From mass-balance expressions for stable Cl and $^{36}\text{Cl}/\text{Cl}$, the site-specific end-member Cl concentrations of the Pleistocene and Holocene proportions of a water sample can be determined from

$$m_{\text{Cl}}^P = \frac{(^{36}\text{Cl}^{\text{meas}} - ^{36}\text{Cl}^H) m_{\text{Cl}}^{\text{meas}}}{f^P (^{36}\text{Cl}^P - ^{36}\text{Cl}^H)} \quad (2a)$$

and

$$m_{\text{Cl}}^H = \frac{(m_{\text{Cl}}^{\text{meas}} - f^P m_{\text{Cl}}^P)}{(1 - f^P)} \quad (2b)$$

where m_{Cl} is Cl concentration; ^{36}Cl is $^{36}\text{Cl}/\text{Cl}$ ratio; the superscripts *meas*, *H*, and *P* indicate the measured value and site-specific end-member values for the Holocene and Pleistocene components, respectively; and other terms are defined elsewhere in the text. Cl concentrations in perched water were 6.8 mg/L at borehole UZ-14 and 3.95 mg/L at borehole SD-7 (Table 2). Based on theoretical reconstructions fitted to packrat-midden data, the $^{36}\text{Cl}/\text{Cl}$ ratio in precipitation was $1,000 \times 10^{-15}$ in the late Pleistocene Epoch and 500×10^{-15} throughout the Holocene Epoch (Fabryka-Martin et al. 1997, Fig. 3-2). Analysis of the $\delta^{18}\text{O}$ data indicates the presence of 47 and 58% Pleistocene water in UZ-14 and SD-7, respectively, to estimate m_{Cl}^P and m_{Cl}^H .

Assuming an average Cl concentration in precipitation of 0.35 mg/L, the estimated Cl concentrations in the Holocene fraction of perched water at SD-7 and UZ-14 imply Holocene percolation fluxes of 8.2 and 7.4 mm/year, respectively (Table 2), as compared to 15 and 8.5 mm/year calculated directly from the measured

Table 2 Measured chloride concentrations and estimated Holocene and Pleistocene chloride concentrations and recharge rates for perched water at boreholes SD-7 and UZ-14

Parameter	Value	
	Borehole SD-7	Borehole UZ-14
<i>Measured values^a</i>		
$\delta^{18}\text{O}$ (per mil)	-13.3	-13.1
Cl (mg/L)	3.95	6.8
$^{36}\text{Cl}/\text{Cl} \times 10^{15}$	612	690
<i>Calculated values</i>		
Pleistocene fraction ^b	0.58	0.47
Cl concentration (mg/L)		
Holocene ^c	7.3	8.0
Pleistocene ^d	1.5	5.5
Flux ^e (mm/year)		
Overall average ^f	15	8.5
Holocene	8.2	7.4
Pleistocene	40.0	10.8

^a Data source: CRWMS M&O (2000a)

^b Calculated based on $\delta^{18}\text{O}$ by the approach described in the text

^c Calculated using Eq. (2b)

^d Calculated using Eq. (2a)

^e Calculated using Eq. (1)

^f Calculated using the measured Cl concentration

perched-water Cl data. Compared to the flux estimates calculated from the measured Cl data, the deconvoluted Holocene flux estimates are more consistent with infiltration rates, estimated for this location by the numerical infiltration model, for the present-day (Holocene) climate (Fig. 4b). The calculated Pleistocene infiltration rates are several times higher than the Holocene rates – 40 mm/year at SD-7 and 11 mm/year at UZ-14 (Table 2) – suggesting that the section at SD-7 is more strongly affected by climatic changes than that at UZ-14.

Evidence for non-local sources of recharge

The groundwater beneath Yucca Mountain is a mixture of groundwater derived from local recharge at Yucca Mountain and groundwater that has flowed beneath Yucca Mountain from upgradient areas. Contour maps of the regional hydraulic heads indicate that possible upgradient sources of groundwater beneath Yucca Mountain include Timber Mountain north of Yucca Mountain and Crater Flat west of Yucca Mountain (Tucci and Burkhardt 1995; Fig. 4); head measurements from the deep carbonate aquifer at Yucca Mountain indicate that upward flow from the deep carbonate aquifer into the volcanic aquifer beneath Yucca Mountain is also possible (Tucci and Burkhardt 1995; Table 2). If upgradient sources of water have mixed with local recharge in the groundwater at Yucca Mountain, and if these upgradient sources have Cl concentrations that are different from the water that has been recharged through Yucca Mountain, then it would be important to compensate for the effects of this mixing before estimating local recharge from the mixed-water chemistry using the CMB method. Compensation would be important because groundwater

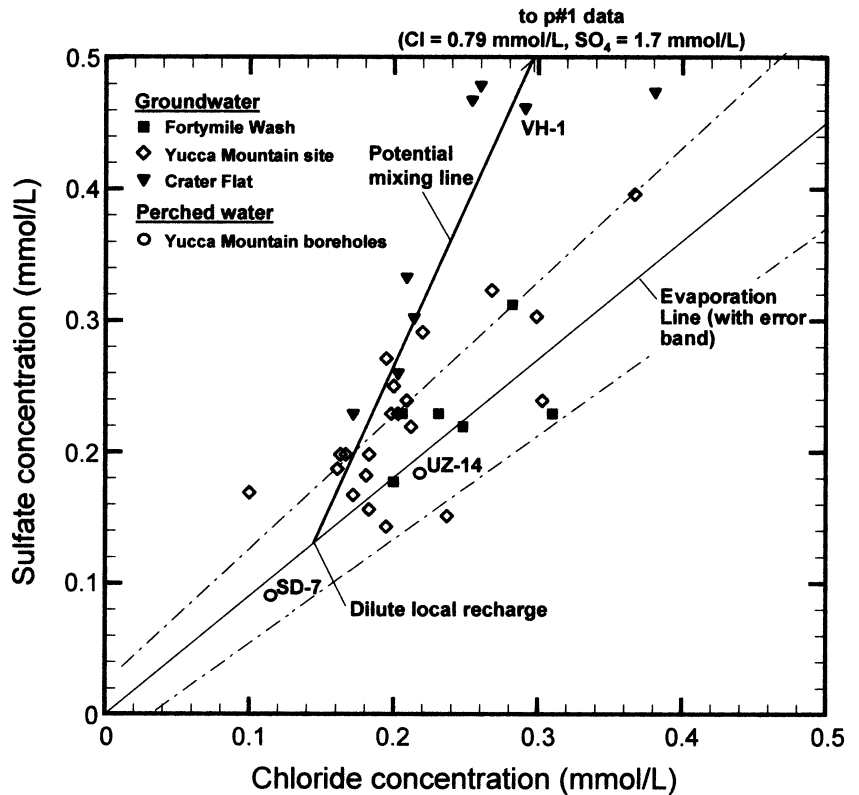
from at least two of these sources, the volcanic aquifer in Crater Flat and the carbonate aquifer beneath Yucca Mountain, has higher Cl concentrations than most Yucca Mountain groundwater samples (Benson and McKinley 1985; Table 1); thus, failure to account for mixing of local recharge with groundwater from these upgradient sources would result in an underestimate of the magnitude of local recharge.

To evaluate possible mixing relations, sulfate (SO_4) and Cl concentrations of groundwater and perched water from the Yucca Mountain area were plotted (Fig. 8). Following methods outlined in CRWMS M&O (2000a), the evaporation trend of precipitation and associated uncertainty limits based on precipitation chemistry for the Kawich Range (McKinley and Oliver 1994, 1995), about 130 km north of Yucca Mountain, are also shown. Groundwater samples with SO_4 and Cl concentrations plotting near this line probably have only meteoric sources of SO_4 and Cl, concentrated to varying degrees by evapotranspiration. Included in this group are two perched-water samples from beneath Yucca Mountain, groundwaters from the vicinity of Fortymile Wash east of Yucca Mountain, and groundwaters from the immediate vicinity of Yucca Mountain itself. However, SO_4/Cl ratios in groundwater from the volcanic aquifer in Crater Flat (for example, VH-1) as well as from the carbonate aquifer that underlies it (for example, p#1) show enrichment in SO_4 relative to the evaporation line (Fig. 8). These waters also have significantly higher SO_4 and Cl concentrations as well as higher SO_4/Cl ratios, as compared to the Yucca Mountain and Fortymile Wash groundwater samples plotted on this figure. Regional sources of sulfur in the saturated zone include sulfide and SO_4 minerals in hydrothermally altered rocks, and gypsum in the rocks above the carbonate aquifer (Winograd and Thordarson 1975).

Based on the discussion above, conservative estimates of local recharge using the CMB method are made by assuming that groundwaters beneath Yucca Mountain with elevated SO_4 concentrations are a mixture of local recharge and these higher-concentration, upgradient end-members (Fig. 8). The Cl concentration of the unmixed, dilute local recharge is estimated to be 0.14 mmol/L (5.0 mg/L), based on the intersection of the meteoric SO_4 -Cl evaporation line with the potential mixing line passing through the data plotted for boreholes p#1, VH-1, and other Crater Flat groundwaters. This crude estimate is roughly the average of the Cl concentrations measured for perched water from boreholes SD-7 and UZ-14 (Fig. 8).

A straightforward application of the CMB equation [Eq. (1)] using a value of 5.0 mg/L for C_s results in an estimated local recharge rate of 12 mm/year. Uncorrected groundwater ^{14}C ages at Yucca Mountain (Benson and McKinley 1985; Table 1) indicate that most of Yucca Mountain groundwater recharged during late Pleistocene or early Holocene times; therefore, the recharge estimate of 12 mm/year is probably more representative of pluvial conditions than of the present dry climate.

Fig. 8 Sulfate and chloride concentrations of groundwater and perched water from the Yucca Mountain area. Forty-mile Wash runoff data are from Savard (1998) and CRWMS M&O (2000a); data for groundwater from the Yucca Mountain area and Crater Flat are from Benson and McKinley (1985) and CRWMS M&O (2000b); perched-water data are reported in Yang et al. (1996)



Atmospheric Radionuclides

Tritium, carbon-14 (^{14}C), and chlorine-36 (^{36}Cl) are standard tools for hydrologists studying water-residence times. These tracers are produced naturally in the atmosphere by cosmogenic processes, and their atmospheric concentrations in the past half-century were augmented dramatically by activities related to nuclear-weapons testing. Application of these tracers at Yucca Mountain is illustrated by the examples presented below.

Tritium

As part of site-characterization activities at Yucca Mountain, tritium has been analyzed in over 800 samples of pore-water fluids extracted from unconsolidated material in shallow surface-based boreholes, from drill core from deep surface-based boreholes, and from ESF drill holes (Yang et al. 1996, 1998; section 6.6.2 in CRWMS M&O 2000a). Analyses are also available for water samples bailed and pumped from perched-water bodies and from the saturated zone. Although the majority of the analyses were not statistically distinguishable from background, detectable levels of tritium (i.e., levels above 25 tritium units) were observed in the Bow Ridge fault zone intersected by the ESF (Fig. 2) and in many pore waters extracted from core samples from surface-based boreholes. These detections occurred within the TCw, PTn, and TSw, and also in some samples from the Tac and Ttp.

Based on tritium peaks observed at depths of 4.5 and 3.5 m in alluvium at boreholes UZ#4 and UZ#7, respectively (Kume and Hammermeister 1990; Loskot and

Hammermeister 1992), the average percolation fluxes at these locations were 35 and 24 mm/year for the period 1963–1984 (Kwicklis et al. 1993). Given the locations of these boreholes in a channel, however, it is conceivable that the tritium peaks were transported to the observed depth shortly after one or two large runoff/infiltration events, rather than representing an annual average. Use of tritium measurements for estimating percolation fluxes elsewhere at Yucca Mountain, however, is complicated by the prevalence of near-surface fracture flow, which leads to the absence of a well-defined profile. Some unsaturated-zone boreholes show several inversions, in which samples with larger tritium concentrations occur below background values in a vertical profile (Yang et al. 1996). These inversions suggest that vertical water percolation through the rock matrix is not the predominant flow mechanism in the unsaturated zone for all stratigraphic units at Yucca Mountain. The occurrence of detectable tritium in waters below non-tritium-bearing water (and hence older water) in a vertical profile is strong evidence for the occurrence of fracture and lateral flow at Yucca Mountain.

Carbon-14

Carbon-14 measurements of borehole gas provide the basis for estimating the infiltration rates for several boreholes penetrating the unsaturated zone. E.P. Weeks (US Geological Survey, personal communication, 1997) applied a model presented in Cook and Solomon (1995) for simultaneous diffusive transport in the gas phase and

convective transport in the liquid phase. The model assumes local equilibrium between the two phases, such that coupled transport is treated using the form of the standard transport equation for single-phase flow, with appropriate redefinition of the coefficients. Results of the simulation indicate that ^{14}C transport in the liquid phase is dominant when the infiltration rate exceeds about 2 mm/year. Assuming piston flow, infiltration rates were computed from measured ^{14}C activities and the estimated volume of water per unit area in storage above the measurement point, by the equation:

$$q = -\lambda V_{UZ} / \ln(^{14}\text{C}_m / 100) \quad (3)$$

where q is the Darcy flux (m/year); λ is the radioactive decay constant for ^{14}C (1.21×10^{-4} /year); V_{UZ} is the volume of water in storage per unit area above the measurement point (m); and $^{14}\text{C}_m$ is the measured ^{14}C activity (in percent modern carbon). This model was used to calculate infiltration rates ranging from 4–9 mm/year for several boreholes at Yucca Mountain. These infiltration rates are characterized by Weeks (1987) as being diffuse because rapid, highly channelized liquid flow might not exchange with the gas phase rapidly enough to maintain the gas/liquid equilibrium assumed by the model; therefore, the gas phase ^{14}C might reflect only the slow-moving, diffuse component of recharge. Although the model assumes vertical flow, some of the deep samples, particularly those associated with perched water, may have been derived predominantly from water moving laterally along the perching layer. If this were the case, the actual flow paths would be longer than the paths assumed by the one-dimensional model, and the actual fluxes would be correspondingly higher.

Chlorine-36

Lower and upper bounds for the site-scale infiltration rate were determined based on the presence of bomb-pulse ^{36}Cl in the deep subsurface. Fast, deep transport of this nuclide to depths as great as 300 m below the surface is controlled by three factors: (1) soil thickness less than 3 m (otherwise the bomb-pulse signal is still largely retained in the soil profile), (2) an infiltration rate sufficient to initiate and sustain fracture flow, and (3) a continuous fracture pathway (Fabryka-Martin et al. 1997). A site-scale transport model indicates that infiltration fluxes of 1–10 mm/year are necessary for even small amounts of bomb-pulse ^{36}Cl to arrive at the sampled locations in less than 50 years, depending on the characteristics of the secondary permeability assumed for the PTn (Fabryka-Martin et al. 1997, Tables 8-2 to 8-4) and on the thickness of the PTn at a particular location (Wolfsberg et al. 2000).

These lower and upper bounds are consistent with natural variations in ^{36}Cl fallout from the atmosphere prior to the nuclear age. Based on analyses of $^{36}\text{Cl}/\text{Cl}$ in local packrat middens that had been dated by ^{14}C (Plummer et al. 1997), the time-variable input of atmospheric ^{36}Cl uses a value of 500×10^{-15} to characterize in-

put throughout the Holocene Epoch, and higher ratios of as much as $1,500 \times 10^{-15}$ to characterize pre-Holocene infiltration (Wolfsberg et al. 2000). Modeling results that best match the ESF data set are consistent with percolation fluxes limited to the range of 1–10 mm/year. Percolation fluxes much less than 1 mm/year are insufficient to induce fracture flow through the densely welded Tiva Canyon and Topopah Spring Tuffs and result in simulated $^{36}\text{Cl}/\text{Cl}$ ratios at the ESF horizon that had experienced considerable radioactive decay compared to the meteoric inputs. Conversely, percolation fluxes greater than 10 mm/year result in short travel times that lead to the dominance of Holocene water that has $^{36}\text{Cl}/\text{Cl}$ ratios typical of this period (near 500×10^{-15}), contrary to the field data.

Watershed Modeling

If water movement from the ground surface to the depth of the potential repository horizon is predominantly vertical, and if the rate at which moisture is removed by processes such as shallow gas-phase circulation is relatively small, then the magnitude and distribution of net infiltration becomes the predominant control on the magnitude and distribution of percolation at depth. The advantage of using infiltration to estimate percolation at depth, compared to other methods described in this paper, is that geographic coverage of the mountain is possible through a relatively large number of shallow boreholes drilled specifically for the purpose of monitoring changes in the moisture status of the unconsolidated surficial material and shallow bedrock, and through detailed mapping of surface soils and bedrock geology.

The numerical model developed to calculate spatially distributed net infiltration at the Yucca Mountain study area is intended to reflect the processes described in the conceptual model of infiltration (Flint et al. 2000). The current conceptual model upon which the numerical model was developed identifies precipitation as the most significant environmental factor controlling net infiltration at Yucca Mountain. Precipitation at Yucca Mountain averages 170 mm/year but is temporally and spatially variable (Hevesi et al. 1992). The depth of infiltration into the soil/bedrock profile fluctuates on a seasonal basis but is greatest in the winter, owing to lower evapotranspiration demands, higher amounts of precipitation, and the accumulation and melting of snow. The second most significant environmental factor controlling net infiltration is soil depth, and when the soil just above the soil/bedrock interface attains near-saturated conditions, fracture flow is initiated in the bedrock, thereby increasing the hydraulic conductivity by several orders of magnitude. Soils exceeding 3–6 m in thickness virtually eliminate infiltration of water to the soil/bedrock interface or deeper except beneath channels (Flint and Flint 1995). The third factor controlling net infiltration is bedrock hydraulic conductivity, and the bedrock at the site varies considerably in both matrix conductivity and degree of fracturing.

The model was used to estimate the temporal and spatial variability of net infiltration (Fig. 4b) for the upper boundary conditions of the unsaturated-zone flow model (Bodvarsson and Bandurraga 1996). It is a pseudo-three-dimensional model with surface routing of runoff in two dimensions. After runoff subsides, the model reverts to separate one-dimensional columns where net infiltration is modeled using a distributed-parameter (Hatton 1998) model approach. The numerical model uses mass-balance processes, measured or stochastically simulated precipitation, the physical setting, and hydrologic properties of the site to approximate the actual conditions at Yucca Mountain. Net infiltration is simulated as precipitation minus change-in-storage minus evapotranspiration minus runoff. Precipitation is measured or stochastically simulated daily; evapotranspiration is simulated daily using a solar-radiation model; and change-in-storage incorporates the physical and hydrologic properties of the site, such as soil-moisture conditions and properties, soil depth, and bulk bedrock permeability (saturated hydraulic conductivity of the matrix and fractures combined) of the underlying geologic formation. The model determines whether field capacity is exceeded by precipitation and whether water drains to the soil/bedrock interface and becomes evapotranspiration or net infiltration. Based on field observation, this is a fairly robust process and net infiltration is easily predicted on the basis of measurements of precipitation and estimates of soil storage capacity. Net infiltration is calculated as the bulk permeability of the underlying bedrock whenever saturated conditions exist directly above the soil/bedrock interface.

Modeled net infiltration at Yucca Mountain varies temporally and spatially, averaging 2.9 mm/year in the site study area and 4.5 mm/year in the potential repository area for the present-day climate (Fig. 4b). This figure illustrates the differences between using a numerical model with many parameters and site characteristics, and using the statistical approach shown in Fig. 4a. The main difference is the spatial detail, and the use of a numerical model allows for the estimation of net infiltration under varying climatic conditions. Spatial and temporal variability of precipitation is the most important factor affecting net infiltration at Yucca Mountain. For example, no infiltration may occur for several years and then 10–20 mm, spatially averaged, may occur in a single year. Also, no net infiltration occurs in an area where the soil is 5 m or greater in thickness; but more than 250 mm may occur in an area where (1) the soil is thin, such as on north-facing slopes, (2) evaporation is low, (3) elevation (and hence precipitation) is high, and (4) the underlying bedrock is permeable. The amount of precipitation alone, however, does not determine net infiltration; timing also must be considered, because, compared to widely spaced precipitation events, more closely spaced precipitation events are more likely to penetrate deeper and result in net infiltration before evapotranspiration reduces the saturation in the soil profile.

Bounds on Moisture Loss by Gas-Flow Processes

Maps of net infiltration determined from soil-zone water budgets assume that no additional moisture is removed below the soil zone by gas-phase processes, such that net-infiltration flux is equivalent to percolation flux and, ultimately, to recharge. In thick unsaturated zones in arid regions, this assumption requires further evaluation. At Yucca Mountain, gas-flow and gas-chemistry studies indicate that subsurface convective gas flow is substantial and that gas residence times within the Tiva Canyon Tuff along Yucca Crest are less than a decade (Thorstenson et al. 1998). Subsurface gas-circulation patterns that arise as a result of temperature- and moisture-induced gas-density differences (E.P. Weeks, US Geological Survey, personal communication, 1997) result in the net removal of moisture from Yucca Mountain, because the air that enters the mountain is dry and the air that leaves the mountain is reasonably assumed to be saturated. Similarly, moisture is removed when dry air enters the mountain during periods of increasing barometric pressure, and moist air leaves during periods of barometric pressure decline.

Small to near-zero temperature gradients within the Tiva Canyon Tuff at boreholes along Yucca Crest (Sass et al. 1988) suggest that heat is removed in the shallow subsurface by processes other than conduction. The maximum evaporation rate in the Tiva Canyon Tuff due to gas-phase processes can be estimated by assuming that all of the upward conductive heat flux estimated for the Topopah Spring Tuff at Yucca Crest (approximately 0.040 J/s/m²) is consumed by evaporation, resulting in the nearly isothermal conditions observed in the Tiva Canyon Tuff. In this case,

$$q_l \times H_v = 0.040 \text{ J/s/m}^2 \quad (4)$$

where q_l is the equivalent evaporated water flux, and H_v is the heat of vaporization (2.45×10^6 J/kg). The resulting equivalent evaporating water flux is 1.6×10^{-8} kg/s/m², or 0.5 mm/year.

The map of infiltration determined from soil water-balance studies indicates that shallow net infiltration along Yucca Crest is 3–10 mm/year (Fig. 4b). Therefore, deeper gas-phase processes potentially remove at most about 5–17% of this moisture. Elsewhere at Yucca Mountain, net infiltration is lower, but gas circulation and evaporation rates may also be lower because the pronounced topographic relief that drives gas-phase circulation is absent.

Comparison of Methods

A wide range of recharge values results from the various methods that have been used at Yucca Mountain (Fig. 9). Generally, these estimates are calculations of percolation flux through the unsaturated zone, although several, for example, Maxey-Eakin, directly estimate recharge to the groundwater system, assuming negligible travel time through the unsaturated zone. For purposes of compari-

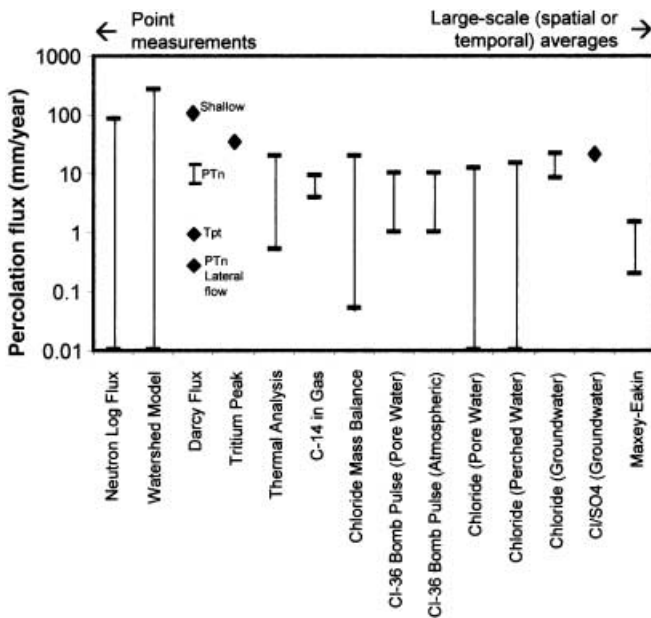


Fig. 9 Comparison of percolation fluxes estimated by various methods. A bar represents a range of estimates, and each point represents a single estimate

son, these estimates are all assumed to be percolation flux rates through the unsaturated zone in millimeters per year in Fig. 9, which indicates the values noted in the above discussion, either as ranges of values or as single estimates. The methods are generally arranged in order of the integrated depth or temporal scale that the method addresses, and the flux is on a log scale. Shallow point measurements are shown on the left part of the x axis and address surface processes generally acting on a yearly to decadal scale, or reflect processes in a single topographic feature, such as a wash or ridge top. Measurements deeper in the mountain, or those integrating entire boreholes, reflect an integration of time and space due to unsaturated-flow processes, stratigraphic influences, and differences in fracture/matrix interaction within the various lithostratigraphic units. These are shown on the right part of the x-axis. Some methods, such as those using perched-water chemistry, incorporate various percentages of water that may be thousands of years old. Different methods reflect combinations of mechanisms that are operating, such as the Maxey-Eakin approach. This approach was developed using basins dominated by alluvial fill, with recharge occurring in the upland areas, but it integrates all mechanisms on the assumption that all are a function of the precipitation. Thus, although the flux values differ substantially, all may generally be correct if the mechanism that is operating and the scale at which it operates are taken into consideration. A summary of the methods, their associated approach, the scale at which the method is applied, and the strengths and limitations of each method is presented in Table 3.

The timing of recharge in the desert southwest, and particularly at Yucca Mountain with its considerable ver-

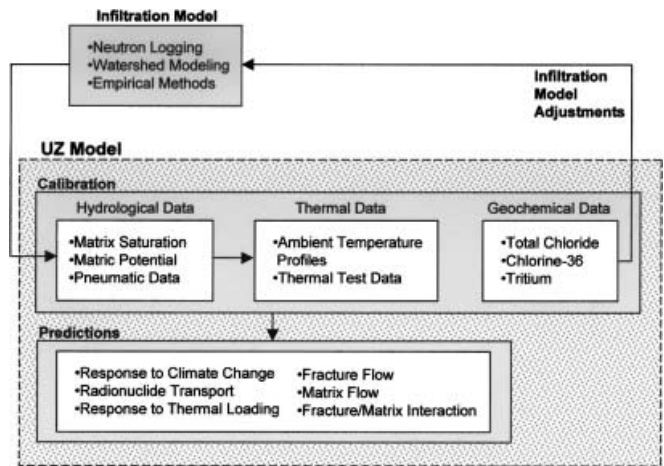


Fig. 10 How the various hydrological, thermal, and geochemical methods are used in the UZ Model to estimate integrated 3-D recharge/percolation flux

tical heterogeneity, is a significant part of the determination of recharge and should be factored into estimates at any site. Quite likely all extremes of the fluxes summarized in Fig. 9 occur somewhere in time and space at Yucca Mountain. The methods and discussions presented here indicate that no single method or single location adequately characterizes flux in such a heterogeneous system.

Integrated Recharge Model

The preceding sections review the various methods used to estimate recharge at the Yucca Mountain site. All of these methods produce estimates that are highly approximate, but complementary rather than redundant because they are based on vastly different assumptions. The three-dimensional unsaturated-zone flow and transport model (UZ Model; Flint et al. 2001b) is a 100,000-grid-block, dual-continuum model that uses the code TOUGH2 (Pruess 1991). This code employs an integrated finite-difference method and multidimensional geometry to calculate coupled flow and transport of air, water, and heat using Richards-equation-based flow.

The UZ Model incorporates the various approaches for estimating recharge – directly or corroboratively – into a unified model, for the best-available estimate of spatial variability in recharge and percolation flux at Yucca Mountain (Fig. 10). The UZ Model uses a variety of hydrologic, thermal, and geochemical information in the analysis of recharge and percolation flux, as discussed below.

Hydrological Data

The UZ Model uses Darcy's law to correlate hydraulic conductivity with liquid and gas fluxes. In this way, the Darcian approach (described earlier) is fully integrated

Table 3 Summary of methods for estimating recharge at Yucca Mountain, including strengths and limitations of each method

Recharge estimation method	Scale and approach	Model parameters	Strengths	Limitations
Numerical model based on Darcy's law through the Richard's equation	Site scale. Flux is determined by best matches between observed and predicted saturations and water potentials	Rock hydraulic properties as a function of saturation or water potential; measured saturations and water potentials	Parameter-estimation methods in numerical model can provide quantitative measures of uncertainty in the estimated parameters; model can be 1-, 2- or 3-D	Scarcity of site-specific hydraulic-conductivity data; measured saturations or water potentials may not reflect fracture-flow component; difficult to obtain accurate water-potential measurements in rocks at low saturations; requires assumption of steady state; provides non-unique solutions
Direct calculation of flux from Darcy's law	Borehole scale. Uses measure of in-situ water potential and unsaturated hydraulic conductivity to estimate point fluxes	Estimated functional relationships between effective hydraulic conductivity and measured saturations or water potentials	Can obtain continuous profiles of flux along a borehole; method does not require assumption of steady state between measurement points	Scarcity of site-specific hydraulic-conductivity data; measured saturations or water potentials may not reflect fracture-flow component; difficult to obtain accurate water-potential measurements in rocks at low saturations; limited to 1-D analyses (and inferences about water flow in the second dimension)
Neutron moisture monitoring	Borehole scale. Flux is determined from measured increase in water content below zone of evapotranspiration	Monitoring of moisture profiles extending below zone of evapotranspiration	Flux is directly measured, including its temporal variations during the period of monitoring; mechanisms are investigated at topographic scale	Each monitored hole represents only a point estimate; labor intensive due to need for long-term monitoring; method may be insensitive to fracture flow; proper borehole construction is critical in order to avoid leakage along casing; limited to 1-D analyses (and inferences about water flow in the second dimension)
Inverse models to match thermal profiles in boreholes	Borehole scale. Flux is determined by best matches between observed and simulated temperature profiles	Measured temperature-versus-depth profiles; thermal conductivity for each layer as a function of saturation	Flux estimate averaged over length of borehole; method sensitive to mass flux rather than velocity, so responds to fracture flow as well as to matrix flow; thermal conductivity insensitive to saturation and water potential	Must assume steady state; high-precision and accurate temperature logs are critical; each monitored hole represents only a point estimate; temperature profiles can be affected by gas-phase as well as liquid-phase flow processes
Modified Maxey-Eakin transfer method	Site or regional scale. Recharge is estimated as a proportion of spatially distributed precipitation	Average annual precipitation across study area	Can obtain spatial distribution of recharge; input data are usually readily available and can be estimated for those areas for which precipitation data are missing	Annual precipitation is highly variable in arid areas, and the proportion that becomes recharge is a non-linear function of the precipitation; method is empirical, developed for basin or watershed scale rather than point scale

Table 3 Continued

Recharge estimation method	Scale and approach	Model parameters	Strengths	Limitations
Chloride (Cl) mass balance	Point scale for pore waters, watershed scale for perched water, basin scale for groundwater. Flux estimated based on extent to which Cl concentration increases due to evapotranspiration	Cl deposition rate, measured Cl concentrations in subsurface waters	Based on simple concept; excellent surrogate for infiltration rate; few parameters are needed; analyses are easy to make	Many underlying assumptions of method are not completely valid for fractured rock; difficult to extract pore water from densely welded rocks or rocks with low water contents; measured concentration may not be representative of fracture fluids, which can bypass matrix; need large database of pore-water analyses in order to establish clear trends; Cl deposition rate may have been different in past; runoff need to be considered in areas with pronounced relief
Global fallout radionuclides (tritium, carbon-14, chlorine-36)	Point scale for pore waters, watershed scale for perched water, basin scale for groundwater. Estimated flux based on penetration depth and half-life	Measured isotopic concentrations or specific activities in subsurface waters	Detection of young waters using fallout tritium, ^{14}C or ^{36}Cl is well established in hydrologic community; useful for testing specific hypotheses about role of fractures and faults in water movement	Not a direct measure of flux; bounding fluxes must be determined indirectly using numerical model; model results are very sensitive to values assumed for fracture-matrix interactions; tritium requires low detection method; fallout ^{36}Cl not always readily distinguishable from natural ^{36}Cl ; interpretation of ^{14}C concentrations measured in unsaturated zone rarely straightforward
Natural atmospheric radionuclides (carbon-14, chlorine-36)	Point scale for pore waters, watershed scale for perched water, basin scale for groundwater. Flux calculated from residence time of water inferred from radionuclide concentration	Measured isotopic concentrations or specific activities in subsurface waters	^{14}C dating is well established in groundwater studies and age-dating models are well documented; residence times based on ^{36}Cl are grossly qualitative, but useful for testing specific hypotheses about rates and mechanisms of water movement	Not a direct measure of flux; bounding fluxes must be determined indirectly using numerical model; long-term temporal variations in ^{36}Cl not firmly established; interpretation of ^{14}C concentrations measured in unsaturated zone rarely straightforward
Perched-water chemistry, including isotopes	Watershed scale. Residence time inferred from measured chemical or isotopic species for which temporal variations can be established	Major-ion chemistry and isotopic data from borehole tapping the perched body	Integrated signal; data are usually readily available; useful for testing or ruling out specific hypotheses about water origins	Uncertainty about origin and lateral extent of each perched-water body, and whether it is a relict of past climate, or still being fed under today's climate; temporal variations in measured species often not firmly established

Table 3 Continued

Recharge estimation method	Scale and approach	Model parameters	Strengths	Limitations
Saturated-zone water chemistry, including isotopes	Basin and regional scales. Residence time is inferred from measured chemical or isotopic species for which temporal or spatial variations can be established	Major-ion chemistry from boreholes with adequate geographic distribution and known sampling depth	Integrated signal; data are usually readily available; useful for testing or ruling out specific hypotheses about water origins	Sampling depths highly variable from well to well, rarely draw from uppermost part of saturated zone, often tap more than one unit; chemical data trends show scatter. Interpretation complicated by effects of numerous processes operating on different temporal and spatial scales, including reactions in soil zone and mixing of groundwaters; temporal and spatial variations in measured species often not firmly established
Watershed modeling	Watershed and regional scales. Estimate recharge based on infiltration, where infiltration is calculated by mass-balance approach	Spatial and temporal distributions of precipitation, evapotranspiration, soil and bedrock properties (matrix and fracture)	Spatial and temporal distributions of recharge; geographic coverage of site is possible through large number of shallow boreholes; 1-D, 2-D, or 3-D modeling; provides tool for predicting effects of different climate scenarios	Intensive data needs; assumes shallow infiltration is equivalent to recharge

into the UZ Model. The model is calibrated using matrix saturation, moisture tension, pneumatic data, infiltration maps developed from neutron log data, watershed modeling, and other information. In this calibration effort, the infiltration rates at different borehole locations are assumed to be known, and important hydrological parameters such as matrix and fracture permeabilities and moisture-retention curve-fit parameters are adjusted to obtain the best statistical fits with the observed data (Bandurraga and Bodvarsson 1999). The numerical infiltration model has continued to be refined over time; however, the UZ Model runs independently of the infiltration model and assumes a specified spatial distribution of infiltration for a particular climate scenario. The numerical code ITOUGH2 (Finsterle 1999) is used for inverse modeling. ITOUGH2 uses a sophisticated statistical/minimum residual approach to ensure that global minimums are achieved in the calibration process.

Thermal Data

The value of ambient-temperature data from boreholes for estimating deep percolation fluxes and recharge rates results from the dependence of the observed temperature gradient on the vertical liquid-flux rate, averaged over an appropriate volume. The temperature gradient also responds to lateral fluid flow. Key modeling parameters are the effective thermal conductivity for each unit,

which is a strong function of the lithophysical porosity in lithophysical-rich geological units. The UZ Model compares its computed temperature gradients with observed borehole data, and parameters are adjusted as appropriate until reasonable matches with all of the available data are achieved (Wu et al. 1999). The ambient-temperature data are especially useful, because these data are sensitive only to the total water flux and insensitive to fluxes in the separate fracture and matrix continua.

Geochemical Data

Geochemical characteristics of subsurface waters are used in the UZ Model to calibrate the various aspects of the model with respect to recharge, percolation flux, and fast flow paths. Each of these is described below.

Chloride

Chloride concentrations measured for matrix pore waters extracted from drill cores are used to estimate total recharge and potential lateral flow within selected units. Because the Cl signature in recharging water is very sensitive to the infiltration rate, a comparison between the observed Cl concentrations and those predicted using the UZ Model and infiltration maps (based upon neutron logging and watershed modeling) yield valuable information regarding the reliability of the infiltration maps

and the inference of lateral flow (Sonnenthal and Bodvarsson 1999). These UZ Model studies suggest that either a large component of lateral flow must be present in the PTn unit or the infiltration model overestimates infiltration rates at the crest of Yucca Mountain (Sonnenthal and Bodvarsson 1999). Because Cl concentrations are measured for matrix pore waters, they might not be representative of Cl concentrations in water in fast fracture-flow paths. It is postulated, however, that Cl concentrations in the matrix reflect the total (fracture and matrix) percolation flux at depth averaged over tens of thousands of years, in part because water percolating along fractures is expected to convert to matrix flow where fracture paths terminate at stratigraphic contacts.

Fast-flow indicators (chlorine-36 and tritium)

Considerable effort has been devoted to the measurements of ^{36}Cl and tritium. As mentioned earlier, the presence of bomb pulse ^{36}Cl and tritium suggests very fast fracture flow. Data collected and analyzed by Fabryka-Martin et al. (1997) indicate that such fast flow paths are primarily associated with known faults, and the UZ Model was calibrated using this information (Fairley and Wu 1997; Wolfsberg et al. 2000; Y.S. Wu, Lawrence Berkeley Laboratory, personal communication, 2001). The limited amount of available tritium data and uncertainties regarding the effective detection limit for these measurements have resulted in these data not being used explicitly in the UZ Model. Nonetheless, the conceptual model of fast pathways developed on the basis of the detection of bomb-pulse isotopes at depth has been incorporated into the UZ Model.

Non-bomb-pulse chlorine-36

The non-bomb-pulse ^{36}Cl data are used in the UZ Model to indicate the age of the pore water and estimate the travel time from the surface to the sample location. Various analytical and numerical methods were used in the analysis, as described by Sonnenthal and Bodvarsson (1999). The utility of this data set is limited by extensive scattering in some of the data, perhaps resulting from the sensitivity of these measurements to sample preparation, or perhaps a true reflection of in-situ variability of water chemistry on the scale of decimeters.

Carbon-14

Carbon-14 data are used in the UZ Model to estimate percolation flux and recharge, based on an approach described in the above section on moisture loss by gas-flow processes. Moridis et al. (1997) developed a very general framework for total carbon speciation and then applied the model to data from Yucca Mountain boreholes to estimate percolation flux. Although this approach is quite appropriate and relevant for process modeling, uncertainties about sample contamination, isotopic exchange, and interpretation of ^{14}C data for pore waters from the

Yucca Mountain site limit the direct use of these data in the UZ Model.

Model Summary

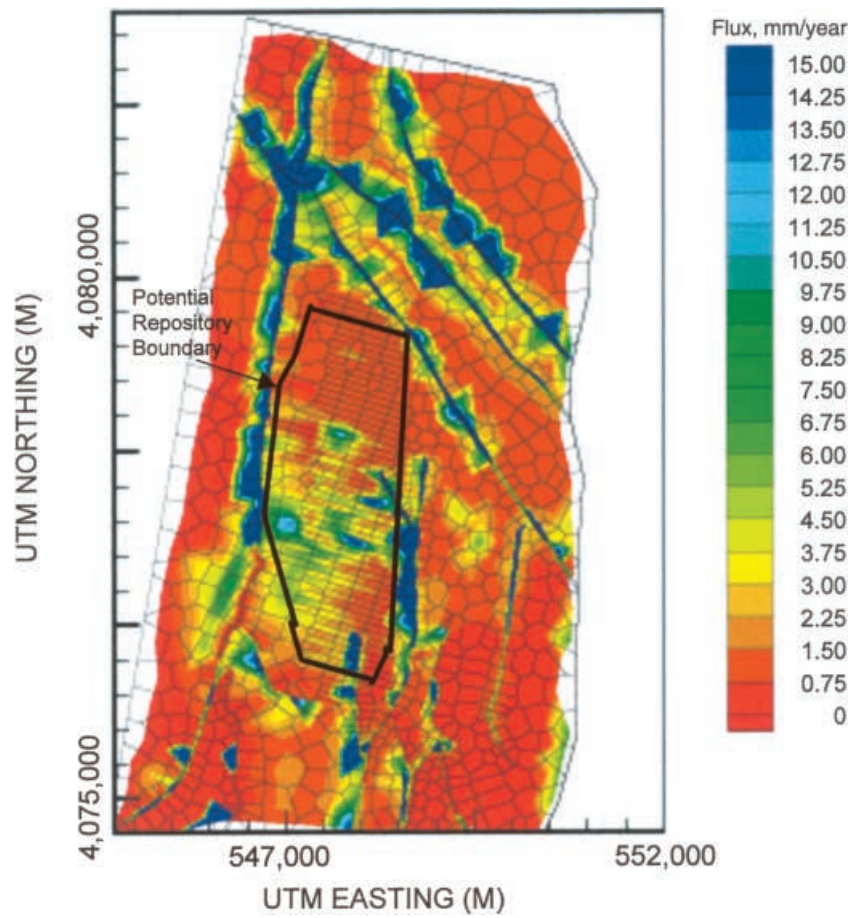
The UZ Model is a vehicle for integrating all of the significant flow processes and mechanisms operating in the unsaturated zone. As a result, the estimated recharge to the water table underlying Yucca Mountain (Fig. 11) differs greatly from the pattern of shallow net infiltration shown in Fig. 4b. The three-dimensional UZ Model simulation in Fig. 11 shows a range of fluxes from 0–15 mm/year, compared to approximately 0–50 mm/year over the same area in Fig. 4b. High fluxes occur in the fault zones at the water table (Fig. 11), whereas surface infiltration is the greatest along the ridge tops and in the larger channels (Fig. 4b). This difference shows how infiltrating moisture is redistributed as a result of low-permeability zeolitic tuffs at depth that cause considerable lateral flow along perching layers, even under the assumed steady-state flow conditions. The UZ Model predicts that most recharge reaches the underlying groundwater by flowing laterally along perching layers or by being channeled through high-permeability vitric tuffs or along faults.

As evident from the discussion above, the UZ Model greatly benefits from the wide variety of hydrological, thermal, and geochemical data available to constrain the model. Preliminary infiltration estimates were about 0.1 mm/year (Flint et al. 2001a), justified on the basis of the widely held assumption that lack of saturation in the TSw unit indicates that fracture flow does not occur and that the infiltration rate therefore does not exceed the unsaturated hydraulic conductivity of that unit at the observed saturation. The credibility and reliability of the present-day UZ Model, which uses infiltration rates more than an order of magnitude higher than earlier estimates, are dependent on the fact that these rates are supported by multiple independent lines of evidence, as well as on the quality and quantity of data that have been collected at Yucca Mountain.

General Discussion and Conclusions

Yucca Mountain has features and characteristics that have made recharge challenging to characterize, especially over time scales relevant to the long-term isolation of high-level nuclear waste (10^3 – 10^5 years). Like other sites in the arid southwest with thick unsaturated zones, water in the unsaturated zone has accumulated from net infiltration over thousands of years. Some water in the deep unsaturated zone infiltrated under climatic conditions quite different from those that exist at present. Additionally, the presence of fractures and faults, the relatively complex hydrostratigraphy, and the pronounced topographic relief of Yucca Mountain have sometimes complicated the direct application of methods originally developed to characterize net infiltration and recharge in simpler hydrologic settings.

Fig. 11 Percolation flux (recharge) at the saturated zone using present-day infiltration as the upper boundary condition in the UZ Model



A variety of methods has been used to estimate net infiltration and recharge at Yucca Mountain (Table 3). These methods produce estimates of flux that reflect different spatial and temporal scales; have different data requirements, strengths, and limitations; and have varying sensitivity to water flux in fractures.

Studies of soil water balance and related models have resulted in detailed maps of net infiltration for the present climate. These maps show temporally averaged net infiltration to be spatially variable and to average 4.5 and 2.9 mm/year over the potential repository area and the larger general study area (Fig. 1b), respectively. The spatial distribution of net infiltration has been largely corroborated by equally detailed estimates of net infiltration from the CMB method using pore-water Cl concentrations measured in rocks sampled from the tunnels at Yucca Mountain. Three-dimensional numerical models of the water movement in the unsaturated zone have also been successful in reproducing measured water potential and saturation data from deep boreholes using the distribution of net infiltration determined from studies of soil water balance. Because of their reliance on measurements made in the rock matrix, each of these three approaches – soil water balance, pore-water CMB method, and Darcy equation-based numerical models – potentially underestimates the fracture component of percolation flux in the densely welded tuffs. However, the three

methods also produce compatible results in the nonwelded tuffs, where fractures are sparse and poorly connected (except in fault zones), such that water flow may reasonably be assumed to be predominantly through the rock matrix. The agreement among these methods in the nonwelded tuffs attests to the general reliability of the percolation-flux estimates.

Numerical models that attempt to reproduce the distribution of bomb-pulse and non-bomb-pulse ^{36}Cl measured along tunnels at Yucca Mountain are able to constrain the likely range of average flux to 1–10 mm/year and to incorporate important geologic and hydrologic factors that control the distribution of ^{36}Cl in the subsurface. Transport models of ^{14}C in the liquid phase that allow for the exchange of ^{14}C with the gas phase produce estimates of flux ranging from 4–9 mm/year. Although infiltration estimates from the ^{14}C modeling study do not always correlate spatially with infiltration estimates from the study of soil water balance, the great depth of many of the ^{14}C data used in the modeling study and the increasing potential for lateral flow at these depths may have obscured correlations with infiltration estimates based on shallower data.

Numerical models that calculate percolation flux by trial-and-error matches to borehole temperature data provide estimates of flux that range from 0.5–20 mm/year, with fluxes in the vicinity of the repository that generally

range from 5–12 mm/year. The overall pattern of infiltration variations inferred from the borehole-temperature analysis is similar to the distribution of net infiltration based on soil water balances, but the former has higher average values. Part of the discrepancy between the water-balance and temperature-based flux estimates may be that decreases in the conductive heat flux may have been caused by gas-phase heat-transfer processes not considered explicitly in the numerical models, in which case these effects could have mistakenly been attributed to water-flow processes.

Numerical models of Cl movement that consider climate change show that the more dilute Cl concentrations deep in the mountain are plausibly associated with water that infiltrated during past climates. A simple mixing model was used to estimate the fractions of Pleistocene and Holocene infiltration in deep perched water from stable-isotope characteristics. Results indicate that the measured Cl concentrations of perched waters agree well with present-day infiltration rates estimated from soil water-balance methods, once one accounts for the effects of pluvial infiltration. The agreement between net infiltration rates estimated from soil water-balance studies and estimates of Holocene infiltration from perched-water Cl data is significant, because the perched water is likely to include any water that moved to depth along fractures that may have been missed by shallower measurements; the agreement between the two infiltration estimates suggests that the amount of fracture flow that is not accounted for is small. Also, despite the relatively short duration of the study, the perched-water data indicate that the soil water-balance study produces infiltration estimates that are representative of the long-term Holocene climate.

The application of the CMB method to groundwater beneath Yucca Mountain results in a recharge estimate of 8.5 mm/year for an average groundwater Cl concentration of 7 mg/L. A groundwater mixing model that considers the potential mixing of high-Cl, upgradient groundwater with local recharge beneath Yucca Mountain was used to estimate a Cl concentration of 5 mg/L for the local recharge component, with a corresponding infiltration rate of 12 mm/year. Uncorrected ^{14}C ages indicate that groundwater beneath Yucca Mountain infiltrated during the late Pleistocene Epoch, so these flux estimates reflect the wetter conditions that existed at that time. The CMB-based infiltration estimates assume that total Cl deposition rates during Pleistocene time were the same as those estimated for the present climate.

The UZ Model integrates the inputs from several of these studies. Model results suggest that heterogeneity associated with the distribution of low-permeability zeolitic tuffs in the deep unsaturated zone results in considerable lateral flow along perching layers. Primarily because of deep lateral flow, the distribution of recharge to the saturated zone differs considerably from the distribution of shallow net infiltration, even under the assumed steady-state flow conditions. The UZ Model predicts that most recharge reaches the underlying ground-

water by flowing laterally along perching layers or by being channeled through high-permeability vitric tuffs or along faults.

The factors contributing to recharge at Yucca Mountain include variable precipitation, topography, and soil depth; and a thick, layered, unsaturated zone with highly variable properties, including fractures and faults. These factors result in a spatially variable influence on the timing of recharge to the saturated zone, from less than a year to thousands of years, and, as a result, approaches used to characterize the recharge at this site require the careful consideration of spatial and temporal scales.

References

- Ahlers CF, Bandurraga TM, Bodvarsson GS, Chen G, Finsterle S, Wu YS (1995) Summary of model calibration and sensitivity studies using the LBNL/USGS three-dimensional unsaturated zone site-scale model. Yucca Mountain Project Milestone 3GLM107 M, Lawrence Berkeley National Laboratory, Berkeley, California
- Bandurraga TM, Bodvarsson GS (1999) Calibrating hydrogeologic parameters for the 3-D site-scale unsaturated zone model of Yucca Mountain, Nevada. *J Contam Hydrol* 38:25–46
- Bandurraga TM, Finsterle S, Bodvarsson GS (1996) Saturation and capillary pressure analysis. In: Bodvarsson GS, Bandurraga TM (eds) Development and calibration of the three-dimensional site-scale unsaturated zone model of Yucca Mountain, Nevada. Yucca Mountain Project Milestone OBO2, Lawrence Berkeley National Laboratory Rep LBNL-39315, Chap 3, Lawrence Berkeley National Laboratory, Berkeley, California
- Benson LV, Klieforth H (1989) Stable isotopes in precipitation and ground water in the Yucca Mountain region, southern Nevada: paleoclimatic implications. In: Peterson DH (ed) Geophysical monograph 55: aspects of climate variability in the Pacific and the Western Americas. American Geophysical Union, Washington, DC, pp 41–57
- Benson LV, McKinley PW (1985) Chemical composition of ground water in the Yucca Mountain area, Nevada, 1971–84. USGS Open-File Rep 85–484, 10 pp
- Bodvarsson GS, Bandurraga TM (eds) (1996) Development and calibration of the three-dimensional site-scale unsaturated-zone model of Yucca Mountain, Nevada. Yucca Mountain Project Milestone OBO2, Lawrence Berkeley National Laboratory Rep LBNL-39315, Lawrence Berkeley National Laboratory, Berkeley, California
- Buesch DC, Spengler RW, Moyer TC, Geslin JK (1996) Proposed stratigraphic nomenclature and macroscopic identification of lithostratigraphic units of the Paintbrush Group exposed at Yucca Mountain, Nevada. USGS Open-File Rep 94–469, 45 pp
- Cook PG, Solomon DK (1995) The transport of atmospheric trace gases to the water table: implications for groundwater dating with chlorofluorocarbons and Krypton-85. *Water Resour Res* 31(2):263–270
- CRWMS M+O (Civilian Radioactive Waste Management System Managing and Operations Contractor) (2000a) Analysis of geochemical data for the unsaturated zone. Rep ANL-NBS-HS-000017, Rev 00, CRWMS M&O, Las Vegas, Nevada
- CRWMS M+O (Civilian Radioactive Waste Management System Managing and Operations Contractor) (2000b) Geochemical and isotopic constraints on groundwater flow directions, mixing, and recharge at Yucca Mountain, Nevada. Rep ANL-NBS-HS-000021, Rev 00, CRWMS M&O, Las Vegas, Nevada
- Dettinger MD (1989) Reconnaissance estimates of natural recharge to desert basins in Nevada, USA, by using chloride-balance calculations. *J Hydrol* 106:55–78

- Fabryka-Martin JT, Flint AL, Sweetkind DS, Wolfsberg AV, Levy SS, Roemer GJC, Roach JL, Wolfsberg LE, Duff MC (1997) Evaluation of flow and transport models of Yucca Mountain, based on chlorine-36 studies for FY97. YMP Milestone Rep SP2224M3, Los Alamos National Laboratory, Los Alamos, New Mexico
- Fairley J, Wu YS (1997) Modeling of fast flow and transport pathways in the unsaturated zone using environmental isotopic tracers. In: Bodvarsson GS, Bandurraga TM (eds) The site-scale unsaturated zone model of Yucca Mountain, Nevada, for the viability assessment. Rep LBL-40376, Lawrence Berkeley National Laboratory, Berkeley, California, pp 16–1 to 16–16
- Finsterle S (1999) ITOUGH2 user's guide. LBNL-40040, Lawrence Berkeley National Laboratory, Berkeley, California
- Flint AL, Flint LE (2000) Near surface infiltration monitoring using neutron moisture logging, Yucca Mountain, Nevada. In: Looney B, Falta R (eds) Vadose zone, science and technology solutions. Battelle Press, Columbus, Ohio, pp 457–474
- Flint AL, Flint LE, Hevesi JA, D'Agnesse FA, Faunt CC (2000) Estimation of regional recharge and travel time through the unsaturated zone in arid climates. In: Faybishenko B, Witherspoon P, Benson S (eds) Dynamics of fluids in fractured rock. Geophysical Monogr 122, American Geophysical Union, Washington, DC, pp 115–128
- Flint AL, Flint LE, Bodvarsson GS, Kwicklis EM, Fabryka-Martin JT (2001a) Evolution of the conceptual model of vadose zone hydrology for Yucca Mountain. *J Hydrol* 247(1–2):1–30
- Flint AL, Flint LE, Kwicklis EM, Bodvarsson GS, Fabryka-Martin JM (2001b) Hydrology of Yucca Mountain, Nevada. *Rev Geophys* 39(4):447–470
- Flint LE (1998) Characterization of hydrogeologic units using matrix properties, Yucca Mountain, Nevada. USGS Water-Resour Invest Rep 97–4243
- Flint LE, Flint AL (1995) Shallow infiltration processes at Yucca Mountain – neutron logging data 1984–93. USGS Water-Resour Invest Rep 95–4035
- Hatton T (1998) Catchment scale recharge modeling. In: Zhang L (ed) Part 4. Basics of recharge and discharge. CSIRO, Collingwood, Victoria, Australia
- Hershey R (1989) Hydrogeology and hydrogeochemistry of the Spring Mountains, Clark County, Nevada. Master's Thesis, University of Nevada, Las Vegas
- Hevesi JA, Flint AL (1998) Geostatistical estimates of future recharge for the Death Valley Region. In Proc 9th Int High-Level Radioactive Waste Manage Conf, Las Vegas, Nevada, 11–15 May, American Nuclear Society, LaGrange Park, Illinois, pp 173–177
- Hevesi JA, Flint AL, Istok JD (1992) Precipitation estimation in mountainous terrain using multivariate geostatistics: II. Isohyetal maps. *J Appl Meteorol* 31(7):677–688
- Ingraham NL, Lyles BF, Jacobson RL, Hess JW (1991) Stable isotope study of precipitation and spring discharge in southern Nevada. *J Hydrol* 125:243–258
- Kume J, Hammermeister DP (1990) Geohydrologic data from test hole USW UZ-7, Yucca Mountain area, Nye County, Nevada. US Geol Surv Open-File Rep 88–465
- Kwicklis EM (1999) Analysis of percolation flux based on heat flow estimated in boreholes. In: Rousseau JP, Kwicklis EM, Gillies DC (eds) Hydrogeology of the unsaturated zone, North Ramp area of the Exploratory Studies Facility, Yucca Mountain, Nevada. US Geol Surv Water-Resour Invest Rep 98–4050:184–208
- Kwicklis EM, Flint AL, Healy RW (1993) Estimation of unsaturated zone liquid water flux at borehole UZ #4, UZ #5, UZ #7, and UZ #13, Yucca Mountain, Nevada, from saturation and water potential profiles. In: Proc Topical Meeting on Site Characterization and Model Validation, Focus '93, 26–29 Sept, Las Vegas, Nevada, American Nuclear Society, La Grange Park, Illinois, pp 39–57
- Kwicklis EM, Flint AL, Healy RW (1994) Simulation of flow in the unsaturated zone beneath Pagany Wash, Yucca Mountain. In: Proc 5th Int High-Level Radioactive Waste Management Conf, 22–26 May, Las Vegas, Nevada, American Nuclear Society, La Grange Park, Illinois, pp 2341–2351
- Lichty RW, McKinley PW (1995) Estimates of ground-water recharge rates for two small basins in central Nevada. USGS Water-Resour Invest Rep 94–4104
- Loskot CL, Hammermeister DP (1992) Geohydrologic data from test holes UE-25 UZ #4 and UE-25 UZ #5, Yucca Mountain area, Nye County, Nevada. USGS Open-File Rep 90–369, 56 pp
- Maxey GB, Eakin TE (1950) Ground water in White River Valley, White Pine, Nye, and Lincoln Counties, Nevada. NV State Eng Water Resour Bull 8, 59 pp
- McElroy DL (1993) Soil moisture monitoring results at the radioactive waste management complex of the Idaho National Engineering Laboratory, FY-1993. EGG-WM-11066, EG&G Idaho, Idaho Falls, Idaho, 110 pp
- McKinley PW, Oliver TA (1994) Meteorological, stream-discharge, and water-quality data for 1986 through 1991 from two small basins in central Nevada. USGS Open-File Rep 93–651
- McKinley PW, Oliver TA (1995) Meteorological, stream-discharge, and water-quality data for water year 1992 from two basins in central Nevada. USGS Open-File Rep 94–456
- Moridis GJ, Apps JA, Bodvarsson GS (1997) ¹⁴C data analysis using the UZ model. In: Bodvarsson GS, Bandurraga TM, Wu YS (eds) The site-scale unsaturated zone model for the viability assessment. Rep LBL-40376. Lawrence Berkeley National Laboratory, Berkeley, California
- O'Brien GM (1997) Analysis of aquifer tests conducted in boreholes USW WT-10, UE-25 WT#12, and USW SD-7, 1995–96, Yucca Mountain, Nevada. USGS Water-Resour Invest Rep 96–4293, 36 pp
- Patterson GL (1999) Occurrences of perched water in the vicinity of the Exploratory Studies Facility, North Ramp. In: Rousseau JP, Kwicklis EM, Gillies DC (eds) Hydrogeology of the unsaturated zone, North Ramp area of the Exploratory Studies Facility, Yucca Mountain, Nevada. USGS Water-Resour Invest Rep 98–4050, 244 pp
- Peters RR, Klavetter EA, Hall IJ, Blair SC, Heller PR, Gee GW (1984) Fracture and matrix hydrologic characteristics of tuffaceous materials from Yucca Mountain, Nye County, Nevada. NM Rep SAND84–1471 (UC-70), Sandia National Laboratories, Albuquerque, 63 pp
- Phillips FM (1994) Environmental tracers for water movement in desert soils of the American Southwest. *Soil Sci Soc Am J* 58:15–24
- Plummer MA, Phillips FM, Fabryka-Martin J, Turin HJ, Wigand PE, Sharma P (1997) Chlorine-36 in fossil rat urine: an archive of cosmogenic nuclide deposition during the past 40,000 years. *Science* 277:538–541
- Pruess K (1991) TOUGH2 – a general-purpose numerical simulator for multiphase fluid and heat flow. Rep LBL-29400, Lawrence Berkeley National Laboratory, Berkeley, California, 102 pp
- Sass JH, Lachenbruch AH, Dudley WW Jr, Priest SS, Munroe RJ (1988) Temperature, thermal conductivity, and heat flow near Yucca Mountain, Nevada: some tectonic and hydrologic implications. USGS Open-File Rep 87–649
- Savard CS (1998) Estimated ground-water recharge from streamflow in Fortymile Wash near Yucca Mountain, Nevada. USGS Water-Resour Invest Rep 97-4273
- Scanlon BR, Tyler SW, Wierenga PJ (1997) Hydrologic issues in arid, unsaturated systems and implications for contaminant transport. *Rev Geophys* 35(4):461–490
- Sonnenthal EL, Bodvarsson GS (1999) Constraints on the hydrology of the unsaturated zone at Yucca Mountain, NV, from three-dimensional models of chloride and strontium geochemistry. *J Contam Hydrol* 38(1–3):107–157
- Thorstenson DC, Weeks EP, Hass H, Busenberg E, Plummer LN, Peters CA (1998) Chemistry of unsaturated zone gases sampled in open boreholes at the crest of Yucca Mountain, Nevada: data and basic concepts of chemical and physical processes in the mountain. *Water Resour Res* 34(6):1507–1529

- Tucci P, Burkhardt DJ (1995) Potentiometric-surface map, 1993, Yucca Mountain and vicinity, Nevada. USGS Water-Resour Invest Rep 95-4149, 15 pp
- Weeks EP (1987) Effect of topography on gas flow in unsaturated fractured rock: concepts and observations. In: Evans DD, Nicholson TJ (eds) Flow and transport through unsaturated, fractured rock. Geophysical Monogr 42, American Geophysical Union, Washington DC, pp 165-170
- Weeks EP, Wilson WE (1984) Preliminary evaluation of hydrologic properties of cores of unsaturated tuff, test well USW H-1, Yucca Mountain, Nevada. USGS Water-Resour Invest Rep 84-4193, 30 pp
- Winograd IJ, Thordarson W (1975) Hydrogeologic-hydrochemical framework, south-central Great Basin, Nevada-California, with special reference to the Nevada Test Site. USGS Prof Pap 712-C, 126 pp
- Winograd IJ, Szabo BJ, Coplen TB, Riggs AC (1988) A 250,000-year climate record from Great Basin vein calcite: implications for Milankovitch theory. *Science* 242:1275-1280
- Winograd IJ, Coplen TB, Landwehr JM, Riggs AC, Ludwig KR, Szabo BJ, Kolesar PT, Revesz KM (1992) Continuous 500,000-year climate record from vein calcite in Devils Hole, Nevada. *Science* 258:255-260
- Wolfsberg A, Campbell K, Fabryka-Martin J (2000) Use of chlorine-36 data to evaluate fracture flow and transport models at Yucca Mountain, Nevada. In: Dynamics of fluids in fractured rocks. Geophysical Monogr 122, American Geophysical Union, Washington, DC, pp 349-362
- Wu YS, Haukwa C, Bodvarsson GS (1999) A site-scale model for fluid and heat flow in the unsaturated zone of Yucca Mountain, Nevada. *J Contam Hydrol* 38:185-215
- Yang IC, Rattray GW, Pei Y (1996) Interpretation of chemical and isotopic data from boreholes in the unsaturated zone at Yucca Mountain, Nevada. USGS Water-Resour Invest Rep 96-4058, 58 pp
- Yang IC, Yu P, Rattray GW, Ferarese JS, Ryan JN (1998) Hydrochemical investigations in characterizing the unsaturated zone at Yucca Mountain, Nevada. USGS Water-Resour Invest Rep 98-4132, 57 pp